

EXTRACTION OF INDICATOR DYES INTO IMIDAZOLIUM-BASED
IONIC LIQUIDS

by

Sarah M. Oplawski

A Thesis Submitted in
Partial Fulfillment of the
Requirements for the Degree of

Master of Science

in Chemistry

at

The University of Wisconsin-Milwaukee

May 2014

ABSTRACT
EXTRACTION OF INDICATOR DYES INTO IMIDAZOLIUM-BASED
IONIC LIQUIDS

by

Sarah M. Oplawski

The University of Wisconsin-Milwaukee, 2014
Under the Supervision of Professor Mark L. Dietz

Among the major classes of water pollutants, dyestuffs have proven to be particularly problematic, both in terms of the quantities released to the environment and the difficulties involved in their recovery from aqueous solution. Each year, textile mills worldwide discharge millions of gallons of dye-laden effluents, leading to significant adverse environmental impact as a consequence of the high chemical oxygen demand and toxicity of these effluent streams. For this reason, there has been considerable interest in the development of a means by which to remove dyes from aqueous waste streams. To accomplish this, textile mills generally employ a combination of physical, biological, and chemical methods, many of which are inefficient and expensive. Liquid-liquid extraction employing ionic liquids (ILs), a novel class of organic solvents typically comprising a bulky asymmetric organic cation in combination with any of a wide variety of anions, has the potential to overcome these problems.

In this work, a variety of imidazolium-based ionic liquids were evaluated for their ability to extract representative cationic and anionic dyes from aqueous solution. UV-visible spectrometry was employed to determine the extent to which each dye is extracted from aqueous solution as a function of pH. Ionic liquids incorporating small (*i.e.*, less hydrophobic) cations were found to extract cationic dyes more efficiently than ILs

incorporating larger (*i.e.*, more hydrophobic) cations. Conversely, ILs incorporating large cations extracted anionic dyes more efficiently than those based on small cations. Unfortunately, recovery of the extracted dyes (and thus reuse of the IL) proved difficult. Thus for ionic liquids to realize their full potential as media for dye removal from wastewater, efficient methods for dye stripping must be identified. In addition, more environmentally benign ILs are required to address their inevitable loss to the aqueous phase during the extraction process.

© Copyright by Sarah M. Oplawski, 2014
All Rights Reserved.

TABLE OF CONTENTS

LIST OF FIGURES	vii
LIST OF TABLES	xi
ACKNOWLEDGEMENTS	xii

CHAPTER 1: INTRODUCTION

1.1 Prevalence and Hazards of Dyes in Wastewater	1
1.2 Treatment of Textile Wastewater	3
1.3 Ionic Liquids	10
1.4 Extraction of Dyes from Aqueous Solution With Ionic Liquids	14
1.5 Characteristics of Selected Dyes	18
1.6 References	19

CHAPTER 2: DEVELOPMENT OF AN EXTRACTION PROCEDURE: A STUDY OF DYE DISTRIBUTION IN OCTANOL-WATER SYSTEMS

2.1 Introduction	22
2.2 Experimental	23
2.2.1 Materials	23
2.2.2 Instrumentation	24
2.2.3 Procedures	25
2.3 Results	26
2.4 Discussion	29
2.5 References	29

CHAPTER 3: DEVELOPMENT OF AN EXTRACTION PROCEDURE: EXTRACTION WITH 1-METHYL-3-OCTYLIMIDAZOLIUM HEXAFLUOROPHOSPHATE

3.1 Introduction	31
3.2 Experimental	31
3.2.1 Materials	31
3.2.2 Instrumentation	32
3.2.3 Procedures	33
3.3 Results	34
3.4 Conclusions	35
3.5 References	36

CHAPTER 4: DYE EXTRACTION INTO IONIC LIQUIDS

4.1 Introduction	37
4.2 Experimental	37
4.2.1 Materials	37
4.2.2 Instrumentation	39
4.2.3 Procedures	39
4.3 Results	40
4.3.1 Methylene Blue Extraction	40

4.3.2 Safranin O Extraction	42
4.3.3 Methyl Violet Extraction	45
4.3.4 Methyl Orange Extraction.....	48
4.3.5 Orange G Extraction	52
4.3.6 Thymol Blue Extraction.....	55
4.4 Effect of Viscosity on Extraction Efficiency	59
4.5 Dye Stripping.....	60
4.6 Conclusions.....	62
4.7 References	63
CHAPTER 5: ASSESSMENT OF ENVIRONMENTAL FRIENDLINESS--	
CONCLUSIONS AND RECOMMENDATIONS	
5.1 Assessment of Environmental Friendliness	64
5.2 Recommendations	74
5.3 References	75
APPENDIX A: STRUCTURES OF DYES.....	77
APPENDIX B: NMR DATA.....	83

LIST OF FIGURES

Figure 1.1 Example of chromophore and auxochrome structures in methyl Orange	2
Figure 1.2 Procedures involved in textile manufacturing in a cotton mill.....	4
Figure 1.3 Schematic of a wastewater treatment plant	5
Figure 1.4 Structures of common cation and anion components of ionic liquids.....	12
Figure 1.5 Acesulfame and saccharinate structures	13
Figure 2.1 Apparatus used for octanol-water systems	23
Figure 2.2 Spectrophotometric Schematic	24
Figure 2.3 Distribution ratio of Methyl Orange in an octanol-water system over time.....	27
Figure 2.4 Distribution ratio of Methylene Blue in an octanol-water system over time ...	27
Figure 2.5 Distribution ratio of Safranin O in an octanol-water system over time	28
Figure 2.6 Distribution ratio of Methyl Violet in an octanol-water system over time	28
Figure 3.1 Distribution ratios vs. pH for Thymol Blue from Visser et al.....	35
Figure 3.2 Distribution ratios vs. pH of Thymol Blue	35
Figure 4.1 Calibration curve for Methylene Blue at pH 7	40
Figure 4.2 Methylene Blue	41
Figure 4.3 UV-visible spectrum of Methylene Blue.....	42
Figure 4.4 Distribution coefficient vs. pH for Methylene Blue	42
Figure 4.5 Safranin O.....	43
Figure 4.6 UV-visible spectrum of Safranin O	44
Figure 4.7 Distribution coefficient vs. pH for Safranin O	44
Figure 4.8 Methyl Violet.....	47
Figure 4.9 UV-visible spectrum of Methyl Violet.....	48

Figure 4.10 Distribution coefficient vs. pH for Methyl Violet	48
Figure 4.11 Methyl Orange.....	49
Figure 4.12 UV-visible spectrum of Methyl Orange	50
Figure 4.13 Fractional composition of Methyl Orange (α vs. pH)	50
Figure 4.14 Distribution coefficient vs. pH for Methyl Orange	51
Figure 4.15 Orange G	53
Figure 4.16 UV-visible spectrum of Orange G.....	53
Figure 4.17 Fractional composition of Orange G (α vs. pH).....	54
Figure 4.18 Distribution coefficient vs pH for Orange G.....	54
Figure 4.19 Thymol Blue.....	56
Figure 4.20 Fractional composition of Thymol Blue (α vs. pH)	57
Figure 4.21 UV-visible spectrum of Thymol Blue	57
Figure 4.22 Distribution coefficient vs. pH for Thymol Blue	59
Figure 5.1A NMR spectrum of C ₈ mimPF ₆ in DMSO	66
Figure 5.1B NMR spectrum of Methylene Blue in DMSO	66
Figure 5.1C NMR spectrum of aqueous phase of MB1, pH 2, C ₈ mimPF ₆	67
Figure 5.2 Fluorine-19 spectrum of C ₆ mimPF ₆	68
Figure 5.3 Fluorine-19 spectrum of TB36, pH 7, C ₆ mimPF ₆	69
Figure 5.4 Fluorine-19 spectrum of C ₆ mimTf ₂ N.....	70
Figure 5.5 Fluorine-19 spectrum of MO52, pH 7, C ₆ mimTf ₂ N.....	71
Figure 5.6 Distribution ratio for Methyl Orange in P _{6,6,6,14} ⁺ Cl ⁻	72
Figure 5.7 Distribution ratio for Orange G in P _{6,6,6,14} ⁺ Cl ⁻	73
Figure 5.8 Distribution ratio for Thymol Blue in P _{6,6,6,14} ⁺ Cl ⁻	73

Figure 5.9 Synthesis of 1,3-disubstituted imidazolium	74
Figure A.1 Thymol Blue.....	77
Figure A.2 Acid Blue Dye	77
Figure A.3 Acid Red Dye	77
Figure A.4 Acridine Orange	78
Figure A.5 Nile Blue A.....	78
Figure A.6 Neutral Red.....	78
Figure A.7 Methylene Blue.....	78
Figure A.8 Safranin O.....	79
Figure A.9 Pinacyanol Chloride	79
Figure A.10 Methyl Orange.....	79
Figure A.11 Eosin Yellow	79
Figure A.12 Orange G.....	80
Figure A.13 Acid Yellow RN.....	80
Figure A.14 Acid Brilliant Red B.....	80
Figure A.15 1-(phenylazo)-2-naphthol	80
Figure A.16 4-(nitrophenylazo) resorcinol	81
Figure A.17 1-(2-pyridylazo)-2-naphthol	81
Figure A.18 4-(2-pyridylazo) resorcinol.....	81
Figure A.19 Methyl Red	81
Figure A.20 Methyl Violet 2B	82
Figure B.1 NMR spectrum of C ₆ mimPF ₆ in DMSO.....	83
Figure B.2 NMR spectrum of C ₆ mimTf ₂ N in DMSO	84

Figure B.3 NMR spectrum of C ₈ mimTf ₂ N in DMSO	85
Figure B.4 NMR spectrum of C ₁₀ mimPF ₆ in DMSO	86
Figure B.5 NMR spectrum of Safranin O, pH 7 in DMSO	87
Figure B.6 NMR spectrum of methyl Violet, pH7 in DMSO.....	88
Figure B.7 NMR spectrum of aqueous phase of SO37, pH 7, C ₆ mimPF ₆	89
Figure B.8 NMR spectrum of aqueous phase of MV43, pH 7, C ₆ mimTf ₂ N	90

LIST OF TABLES

Table 1.1 Characteristics of textile wastewater in Malaysia.....	4
Table 2.1 UV-Visible Spectrophotometer Operating Conditions.....	25
Table 2.2 Wavelength of Maximum Absorbance for Dyes	25
Table 2.3 D_{ow} and $\log D$ at Equilibrium Point.....	28
Table 3.1 Wavelengths of Maximum Absorbance	33
Table 4.1 Isosbestic Points.....	39

ACKNOWLEDGEMENTS

I would like to first thank the members of my review committee, Dr. Arnold and Dr. Aldstadt. They have been most patient and kind and I consider myself quite lucky to have them on my committee. I would also like to thank the members of my research group who helped me with finding resources and/or taught me how to utilize certain equipment, namely Sarah Garvey, Abdul Momen, Alan Pawlak, Anna Rud, and James Wankowski.

I have to thank Dr. Mark Dietz profusely for all of his guidance and assistance throughout this process. I have become a better chemist and researcher as a result of his mentorship.

I must also thank my parents, Robert and Mary Oplawski, as well as my fiancé, Ryan Boldt. They, along with some close friends, supported me along the way and gave me the strength I needed to complete this thesis, particularly in the face of adversity.

CHAPTER 1: INTRODUCTION

1.1 Prevalence and Hazards of Dyes in Wastewater

To meet the demands of a growing population, textile mills are increasing in size and number and thus are producing more dye-containing wastewater. As of 2012, more than 100,000 different dyes existed worldwide, and between 700,000 and 1,000,000 tons were produced each year. The textile industry utilizes about 90% of all dyes, while the remaining 10% are used in food, printing, and plastics. Approximately 280,000 tons of textile dyes are discharged through wastewater on a yearly basis worldwide. The greatest amounts come from Asia, with China as the largest producer [1.1].

As shown in Figure 1.1, dyes are organic compounds that incorporate two main groups. The first is a chromophore, whose structure gives the dye its color. It contains conjugated double bonds and a delocalized electron cloud. Typical structures include double-bonded carbons, cyano groups, carbonyl groups, and azo groups (double-bonded nitrogens). The second component is the auxochrome, which gives the dye its color intensity. This is usually an electron-donating group such as an amine, a carboxylic acid, a sulfate, or a hydroxyl group. Azo dyes account for about 65-70% of all dyes produced, and the vast majority of these dyes are used in textiles [1.2]. These dyes have been the focus of many research studies due to their poor biodegradability and the fact that under certain conditions, they can form aromatic amines, which are carcinogenic.

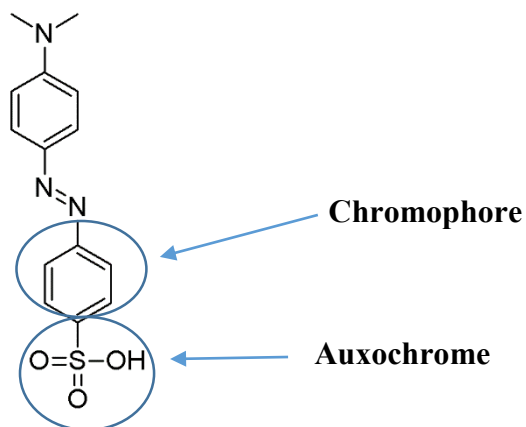


Figure 1.1 Example of chromophore and auxochrome structures in Methyl Orange.

Untreated textile wastewater with dyes present tends to be high in chemical oxygen demand (COD), biochemical oxygen demand (BOD), total organic carbon (TOC), suspended solids (SS), turbidity, and toxicity. The first four factors are often used to characterize the wastewater and establish regulatory levels. The presence of turbidity directly impacts aquatic environments, since clouding of the water will block sunlight and inhibit the photosynthetic ability of water plants [1.1]. The majority of dyes are toxic not only to aquatic environments but also to a wide variety of organisms, ranging from bacteria to humans. For example, in 1998, researchers Bhat and Mathur [1.3] examined the dyes used in synthetic food colors in India. They were stunned to discover that not only were the “safe” dyes potentially dangerous, but also that many food manufacturers were using dyes reserved for textiles! These textile dyes affect nearly all systems and organs, including the liver, kidneys, stomach, heart, spleen, lungs, red blood cells, bones, ovaries, and testes. The so-called “safe” dyes can cause thyroid tumors and a range of allergic reactions. The use of synthetic dyes is unfortunately necessary because natural colors are non-uniform, unstable, expensive, difficult to obtain, and possess various

unpleasant odors [1.3]. Thus, for companies to continue to use inexpensive and readily available synthetic dyes, regulations were imposed.

Government regulations vary widely from country to country and region to region. Wang *et al.* (2011) compared regulations from China, Germany, and the United States, noting that China tends to have stricter and more numerous regulations, including limits for existing factories and for new factories. Also, while Germany has a single set of standards, the United States has three, one for printing, a second for fabric printing, and another for yarn printing. The regulatory limits themselves also vary. For example, the allowable COD (chemical oxygen demand) in China for a new factory is 80 mg/L, while in Germany it is 160 mg/L regardless of factory, and in the United States it is 1.63×10^{-4} mg per ton of fabric. Such variability in regulations is often frustrating to those conducting research as well as those involved in the importing and exporting of goods [1.4]. Nonetheless, what these regulations do indicate is the need for treating wastewater before it is discharged to the environment.

1.2 Treatment of Textile Wastewater

Wastewater is generated at several points throughout the dyeing and washing process and often exhibits varying levels of carbon oxygen demand (COD), biochemical oxygen demand (BOD), suspended solids (SS), and pH, among other factors. Figure 1.2 is a representation of the steps required for textile manufacturing in a cotton mill, and Table 1.1 shows the characteristics of textile wastewater from Malaysia. It is evident that depending upon the process, these characteristics vary greatly. Thus, a satisfactory wastewater treatment process must address these variations, particularly those of pH.

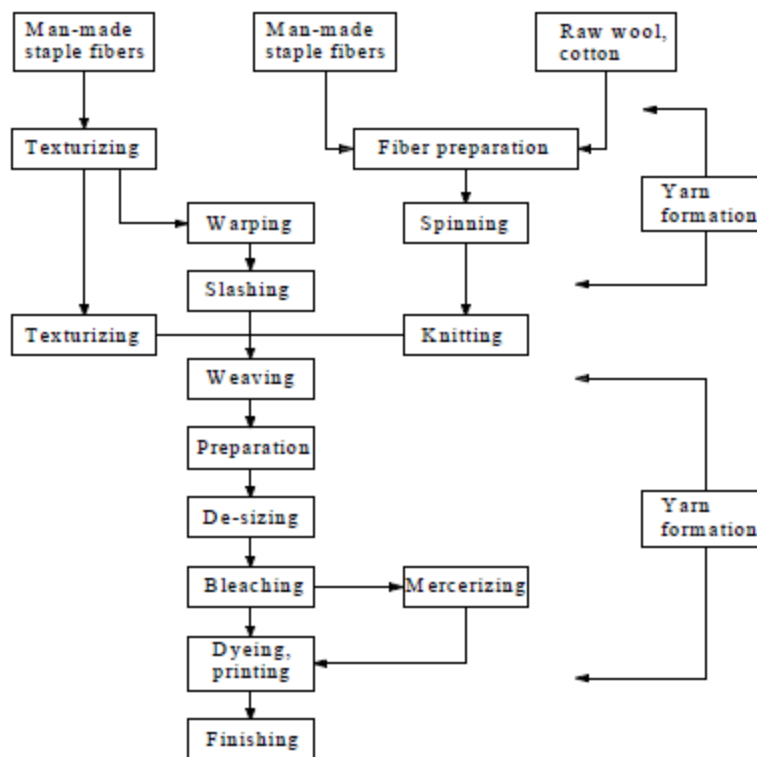


Figure 1.2 Procedures involved in textile manufacturing in a cotton mill [1.4]

Table 1.1 Characteristics of textile wastewater in Malaysia (Adapted from [1.1])

Point of Collection	pH	COD (mg/L)	BOD (mg/L)	SS (mg/L)
Raw wastewater after bleaching and souring	7.4	704	171	644
Raw wastewater after dyeing and finishing	6.9-7.5	14500-21000	n.d.	1840-3000
Raw wastewater after dyeing and finishing	n.d.	2040-3190	n.d.	530-620
After physical, chemical, and biological treatment	3.9-11.4	232-990	n.d.	23-150
After physical and chemical treatment	3.9-11.4	31	n.d.	0.11
After biological treatment	7.0-8.0	200-260	<50	<50

n.d.—no data provided

Most researchers and manufacturers agree that a combination of various treatment processes is necessary. These processes generally fall under three categories: physical,

biological, and chemical. According to Pang and Abdullah (2013), the ideal combination would entail a chemical treatment coupled with a physical treatment, followed by a biological treatment, and finally a physical treatment as a “polishing” step (Figure 1.3).

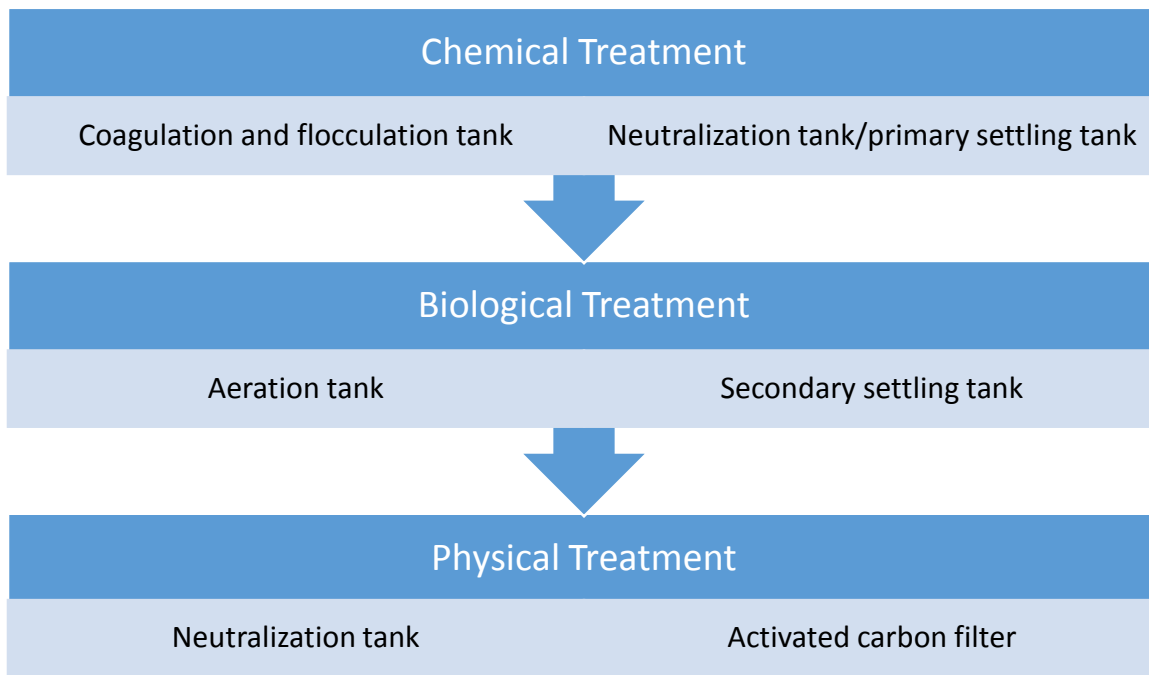


Figure 1.3 Schematic of a wastewater treatment plant (Adapted from [1.1])

Physical treatments typically separate the various components (*e.g.*, solids, dyes, and charged particles) in textile wastewater. There are three primary types of separation: adsorption, ion exchange, and filtration. Adsorption involves the collection of soluble substances on an interface (*e.g.*, activated carbon). This process is efficient for a wide variety of dyes but can be expensive due to the need to regenerate the adsorbent. Ion exchange involves passing the wastewater through an ion exchange column and only removes cations and anions, so while it is effective for charged dyes, it is practically useless for neutral dyes. There is no loss of adsorbent as seen with adsorption and regeneration is required, however. Filtration, which includes microfiltration, ultrafiltration, nanofiltration, and reverse osmosis, requires passing wastewater through a

medium to remove suspended particles. This takes place usually after coagulation or flocculation and tends to be rapid and effective for a variety of dyes. However, this process has several drawbacks, including high cost, the production of sludge (which must also be processed), a short membrane lifetime due to clogging, and the inability to accommodate large volumes of wastewater [1.1].

Biological processes involve the use of microorganisms such as bacteria, plants, or fungi, in aerobic and/or anaerobic conditions to break down the organic compounds present in wastewater and convert them to water and carbon dioxide. Pretreatment is usually required because most dyes, particularly azo dyes, are not readily biodegradable [1.1]. There has been some success in degrading azo dyes in both aerobic and anaerobic conditions [1.1]. Under anaerobic conditions, azo dyes are degraded into aromatic amines, which are also toxic and require further treatment, but a biogas is produced as a byproduct that could potentially be used for fuel and energy [1.1]. Under aerobic conditions, azo dyes are removed from the wastewater by bacteria that possess color-reducing enzymes and converted into sludge. The sludge is often recyclable, but this process is very time-consuming and requires a large amount of acreage. Usually a sequential process involving both conditions is ideal [1.1].

An inherent problem with biological treatment is the sensitivity of many plants and bacteria to toxins. Researchers in India examined wetlands that were constructed solely for these biological processes to determine which plants would be appropriate. Unfortunately, of the ten plants tested, only one managed to survive in various wastewater samples (*phragmites karka*, a type of reed) and researchers concluded that use of this plant was appropriate for, at best, a polishing process. The plants currently

present in these constructed wastelands are rather inefficient since they tend to die off quickly and are unable to process any additional wastewater [1.5].

Chemical processes encompass a wide range of different techniques. They generally include a coagulation/flocculation process as well as an oxidation process. Recently, researchers have been investigating different types of extraction or other chemical processes as an alternative to oxidation reactions. Coagulation and/or flocculation is usually used in conjunction with physical processes as the purpose is to remove suspended particles. A coagulant such as aluminum sulfate, lime, or ferric sulfate is added to a sample and charge neutralization occurs. Neutral particles collide and adhere, forming “flocs”, which can then be removed via sedimentation. This is not time-consuming and can be very efficient, but it is expensive and produces sludge that is difficult to handle and process [1.1].

Oxidation processes are used to generate hydroxide radicals to promote the mineralization of dyes, thus breaking them down into simpler products that can be more readily handled. One major drawback, though, is that the products are usually more toxic than the reactants, so oxidation cannot be used alone [1.1]. There are a variety of ways in which this oxidation can be effected, including Fenton oxidation, ozonation, photocatalytic/sonocatalytic oxidation, and radiolysis. Fenton oxidation uses Fenton’s reagent (Fe^{2+} and hydrogen peroxide) to generate the hydroxide radicals. It is efficient, requires a short amount of time, and is effective for many dyes, but it can be expensive and does produce sludge [1.1]. Researchers Bokare *et al.* attempted a similar reaction using Fe-Ni nanoparticles instead of Fenton’s reagent. They observed the complete degradation of an azo dye, Orange G, in ten minutes but found that these particles are not

suitable for pH levels over 6.0. This is because a hydroxide layer forms on the surface of the nanoparticles and leads to fouling. In addition, the degraded products were aromatic amines, which require further processing [1.2].

Ozonation involves the reaction of ozone with organic matter present in wastewater, either through a direct ozone attack or an indirect free radical attack. This reaction generates hydroxide radicals as intended and is efficient, versatile, and does not produce sludge. Unfortunately, ozone has a rather short half-life (20 minutes) and is not appropriate for insoluble dyes. Photocatalysis uses a metal oxide semiconductor as a catalyst in conjunction with exposure to UV light, while sonocatalysis employs ultrasonic irradiation. Both techniques excite electrons to higher levels, thus leaving gaps in the valence level and prompting water molecules to form hydroxide radicals. Photocatalysis is efficient and versatile but does form by-products and is only appropriate for low dye concentrations. Sonocatalysis is also efficient and versatile and can penetrate water more deeply than photocatalysis, so higher dye concentrations may be used. Radiolysis involves the irradiation of wastewater with gamma rays or electron beams to generate the hydroxide radicals. It is efficient and fast but like filtration processes, can only accommodate small volumes of water. Moreover, it requires a source of radiation [1.1].

One of the more novel chemical treatments that has been investigated involves the use of supercritical water. When water is subjected to the extreme conditions of temperature and pressure that render it supercritical, it tends to have amphoteric properties due to higher concentrations of H_3O^+ and OH^- . This makes it a useful solvent for organic products as well as a reactant for oxidation reactions. In this particular study, this process was used to decompose a textile wastewater sample from a plant in Turkey.

At a temperature of 600°C, the wastewater was decolorized and the dyes present converted to water and carbon dioxide in 150 seconds. This process is costly, but the energy generated could be recycled to lower the cost. More research is needed, but clearly this could constitute a new direction in wastewater treatment [1.6].

Among the other possible types of chemical treatments is liquid-liquid extraction (LLE), in which dye-laden wastewater is contacted with an immiscible organic solvent into which the dyes partition. In 2004, Pandit and Basu employed reverse micelles, “nanometer-sized aggregates of surfactant molecules surrounding a microscopic water core in nonpolar solvents” [1.7], to extract a variety of dyes. (These micelles are reversed because typically, micelles have a hydrophobic core rather than a hydrophilic one.) The dye is extracted from aqueous solutions into the core of the micelles, which then solubilize the dye. The dye-containing phase can then be separated by gravity when the water layer is removed (the layer containing the dye-laden reverse micelles is less dense than water). Removal efficiencies of 70% and higher were observed for the dyes examined. Generally, the removal tended to be higher at lower dye concentrations and at higher surfactant concentrations. While this method has potential, the extracted dye must still be properly disposed [1.7].

Another LLE method, proposed by Muthuraman and Teng (2010), involved the use of a xylene solution of salicylic acid to extract Methyl Violet (a cationic dye) from an aqueous solution. A mixture of salicylic acid and xylene was added to an aqueous dye solution, the resulting combination was mixed and transferred to a separatory funnel, and the aqueous solution was removed for analysis. Extraction was found to be most efficient at a pH level of 6.0, which for reasons not specified, was the highest pH level tested.

Extraction was also more efficient when a higher concentration of salicylic acid was used. One of the advantages of this technique is that the salicylic acid could be reused after the dye was stripped from it, using other stronger acids (*e.g.*, phosphoric, nitric, or acetic acid). Tests showed that the salicylic acid could be used ten more times before the extraction efficiency dropped noticeably (from 96% to 90%). Of course, as with the reverse micelles, the stripped dye still needs to be handled appropriately [1.8].

In 2007, Mahmoud *et al.* examined a variety of more environmentally-friendly solvents for liquid-liquid extraction [1.9]. Specifically, various plant oils (*e.g.*, cottonseed, olive, canola, and sunflower) and used cooking oil were used in an attempt to extract the dye Remazol Brilliant Blue (an anionic dye). Cooking oil was found to be the most efficient solvent for extraction, with similar results being observed for olive oil and much poorer extraction efficiencies being found for the other oils. Interestingly, the extraction efficiency was observed to be correlated with solvent viscosity, suggesting that liquids of higher viscosities may be excellent for media for extraction of dyes, although the reason for this was not indicated.

1.3 Ionic Liquids

The study of ionic liquids constitutes a burgeoning field in a world committed to using more environmentally-friendly practices and products. An ionic liquid (abbreviated “IL”) is generally defined as a fused salt with a melting point less than 100°C [1.10]. The vast majority of ionic liquids also have wide liquid ranges, with melting points as low as -96°C [1.11] and boiling or decomposition points as high as 500°C [1.12]. These ILs are often viscous and non-volatile. It is this low vapor pressure

that can make ILs “greener” than traditionally-used organic solvents, particularly toxic and flammable volatile organic compounds (VOCs) [1.11].

Ionic liquids are sometimes called “designer solvents” due to the significant number of potential cation/anion combinations (up to 10^{18} possibilities [1.13]). Figure 1.4 illustrates some common cations and anions used in the synthesis of ionic liquids, but this list is by no means all-inclusive. In general, IL cations tend to be bulky and asymmetric, as can be seen for the imidazolium, pyridinium, and pyrrolidinium structures. These properties are desirable because they prevent tight crystal packing, thus lowering the melting point. IL anions tend to have delocalized electron clouds in order to reduce any interionic interactions, and can be either bulky (*e.g.*, tosylate or *bis*[(trifluoromethyl)sulfonyl] imide) or simple (*e.g.*, Cl⁻) [1.14] Novel combinations, with a variety of substituted “R” groups on the cation and/or anion, are being synthesized regularly and the library of known ILs continues to grow at a rapid pace.

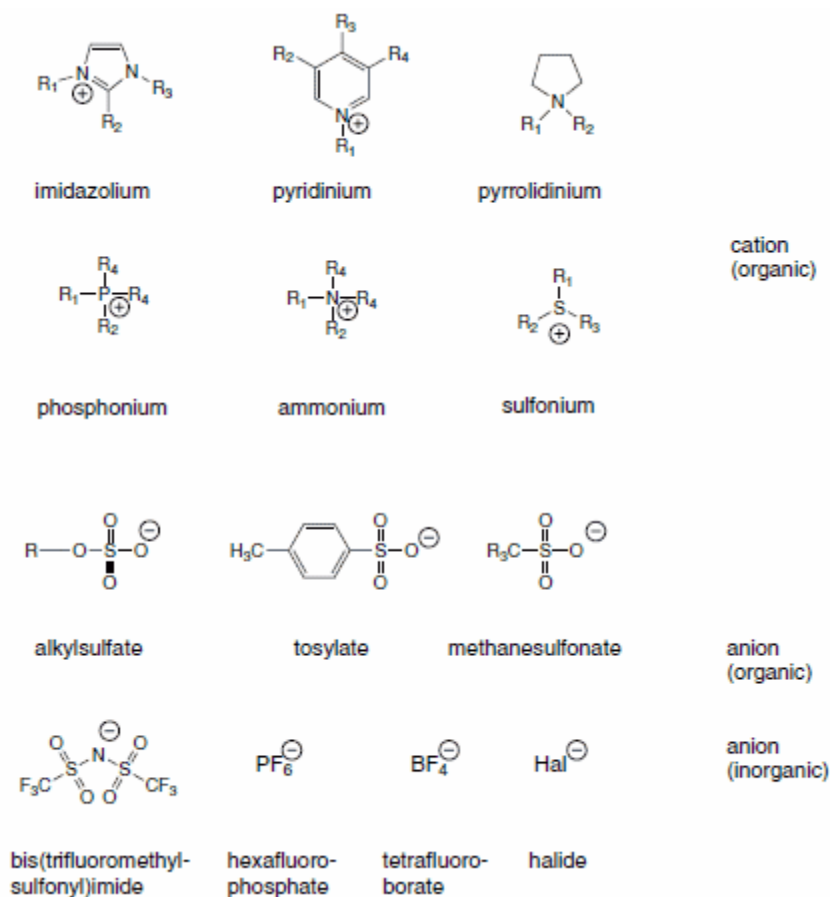


Figure 1.4 Structures of common cation and anion components of ionic liquids

Many have suggested that ionic liquids are green solvents, but this is not always correct. While ionic liquids do exhibit negligible vapor pressure, (thus eliminating fugitive emissions), their cationic and/or anionic constituents are often toxic. For example, the hexafluorophosphate anion, a common constituent of ILs, hydrolyzes to form HF, a decidedly non-green compound. Along these same lines, research has shown that many IL cations lack biodegradability, particularly those with long alkyl chains [1.14, 1.15, 1.16]. Subsequent research has also found that ring planarity may have an effect on the “greenness” of the cation, and that the least toxic cations possess short alkyl

chains and a non-planar ring. The addition of a heteroatom or functional group, such as a nitrile or ester group on an alkyl chain, may also decrease toxicity [1.14, 1.17].

The ionic liquid anion does not seem to affect toxicity to the same extent as the cation, but as noted above, there are some anions that are definitely detrimental to aquatic environments. Any ion possessing one or more fluorine atoms, (*e.g.*, bis [(trifluoromethyl) sulfonyl] imide and hexafluorophosphate), are particularly problematic. Other halogens such as bromine and chlorine are not nearly as toxic but may still react in aquatic environments and be harmful to organisms [1.14]. Research has shown that the more hydrophilic the anion, the less toxic it tends to be [1.17]. Some anions such as acesulfamate and saccharinate (Figure 1.5) tend to have several sites available for enzymatic hydrolysis, which will increase the biodegradability of the overall ionic liquid when paired with a cation possessing short alkyl chains. Therefore, the “ideal” ionic liquid (from the perspective of greenness) would be one that has a cation incorporating a non-planar ring with short alkyl chains and a hydrophilic anion [1.14].



Figure 1.5 Acesulfamate (left) and saccharinate (right) structures

1.4 Extraction of Dyes from Aqueous Solution with Ionic Liquids

A number of studies have been conducted that examined the use of ionic liquids in the extraction of various dyes [1.19-1.24]. For these extractions to be viable, the dye components obviously must partition into the ionic liquid, or organic layer, thus vacating the wastewater (aqueous layer). The remaining wastewater can then be subjected to further treatments or introduced into the environment. The ionic liquid itself must not partition into the aqueous layer in any significant quantities, as the introduction of a harmful cation or anion would be environmentally detrimental. If cation or anion exchange must occur, the cation or anion needs to be environmentally benign.

Quantification of extraction generally involves the calculation of a distribution ratio “D” (expressed as a unit-less number), defined as per Eqn. 1-1, where the concentration of dye in the organic (IL) layer is divided by the concentration of dye in the aqueous layer:

$$D = \frac{[\text{dye}]_{\text{org}}}{[\text{dye}]_{\text{aq}}} \quad (1-1)$$

An extraction is considered efficient when the D value is greater than 10 and inefficient when D is less than 1.0 [1.18].

Several studies have been conducted in which ILs have been used to extract various dyes from water with varying levels of success, (*i.e.*, varying extraction efficiencies). In 2000, Visser *et al.* [1.19] used three imidazolium-based ILs (specifically, 1-butyl-3-methylimidazolium hexafluorophosphate, 1-hexyl-3-methylimidazolium hexafluorophosphate, and 1-octyl-3-methylimidazolium hexafluorophosphate) to extract

the anionic dye Thymol Blue from aqueous solutions at a variety of pH levels ranging from 1.5 to 13. They found distribution ratios ranging from approximately 100 to 1000 for acidic pH and a steep decline to a D_{dye} of less than 1 at a pH of 12 or above [1.19]. Although the pH dependency of extraction is of concern to some due to the need for efficient extraction over a wide pH range (to accommodate the properties of textile wastewater) [1.1], the significant variations in D with pH provides a means by which the extracted dye can be recovered (*i.e.*, stripped) from the IL.

A 2005 study by Vijayaraghavan *et al.* [1.20] examined the extraction of the anionic (*i.e.*, as a sodium salt) forms of Acid Blue and Acid Red into a pyrrolic ionic liquid, specifically *N*-butyl-*N*-methyl pyrrolidinium *bis* [(trifluoromethyl)sulfonyl] imide, abbreviated [P₁₄][Tf₂N]. This particular IL is stable and very hydrophobic. The D values obtained were about 2.0, suggesting that the IL phase was favored, albeit only slightly. If fresh aliquots of IL were repeatedly added, the extraction efficiency for the dyes as high as 95% could be achieved. This method has obvious and significant drawbacks in that fresh IL must be continually added and that some of the IL is lost to the wastewater, necessitating the use of ion exchange resins to recover it prior to discharge of the water to the environment.

In a 2006 communication, Ali *et al.* attempted to extract several different dyes into 1-butyl-3-methylimidazolium hexafluorophosphate (C₄mimPF₆), 1-butyl-3-methylimidazolium tetrafluoroborate (C₄mimBF₄), 1-butyl-3-methylimidazolium bis(trifluoromethylsulfonyl)imide (C₄mimTf₂N), and 1-hexyl-3-methylimidazolium bromide (C₆mimBr) [1.21]. The cationic dyes studied included Acridine Orange, Nile Blue A, Neutral Red, Methylene Blue, Safranin O, and Pinacyanol Chloride, and

extraction efficiencies were as high as 99%. No mechanism of extraction was formally determined, but curiously, the researchers concluded that hydrophobicity of an ionic liquid has no effect on extraction efficiency. This is a claim that would be challenged by at least one subsequent study.

This seemingly contradicting study was conducted by Pei *et al.* in 2007 [1.22]. In this work, four different ionic liquids were used, including C₄mimPF₆, 1-hexyl-3-methylimidazolium hexafluorophosphate (C₆mimPF₆), 1-hexyl-3-methylimidazolium tetrafluoroborate (C₆mimBF₄), and 1-octyl-3-methylimidazolium hexafluorophosphate (C₈mimPF₆). The anionic dyes used were methyl Orange, eosin yellow, and Orange G, and the extractions were carried out over a wide range of pH values. It was observed that the ILs possessing longer alkyl chains were more efficient at extraction, with the highest D values occurring for the C₈mimPF₆ and decreasing as the alkyl chain size decreased. This suggests that the more hydrophobic the IL, the more efficient it is as an extraction solvent. The data also indicated that the neutral form of Methyl Orange has rather poor partitioning (low D's) below its pK_a of 3.46. When the anionic form predominates at pH levels above 4.0, however, the extraction efficiency quickly rises to a plateau. Eosin Yellow, in contrast, exhibited high D values at pH levels below 4 and a steep drop as the pH was increased. Orange G displayed an essentially constant distribution ratio until very basic pHs were reached, at which point D_{dye} declined. The authors speculated that at high pH, the dye is incapable of forming hydrogen bonds with fluorine atoms of the PF₆ anion. This suggests that hydrogen bonding may play a role in the mechanism of dye extraction.

The ionic liquid C₄mimPF₆ was also used in a 2008 study by Li and Xin [1.23], in which the anionic dyes Acid Yellow RN and Acid Brilliant Red B were extracted into the

IL and into a conventional solvent, octanol. The dyes partitioned into the IL much more effectively than into the octanol. For the Acid Yellow, the D value in octanol was 13.6 compared to 130.25 for the IL, while for the Acid Red, the values were 3.0 and 424.8, respectively. These researchers suggested that the ions comprising the ionic liquids act as counter ions, thereby increasing their extracting abilities. It was also determined that acid yellow undergoes anion exchange with the PF_6^- (forming a complex of $[\text{C}_4\text{mim}]_{\text{org}}^+[\text{Dye}]_{\text{org}}^-$ as indicated by comparing NMR spectra of the IL before and after dye contact), making IL recovery difficult after repeated uses due to incorporation of the dye into the IL. The red dye also tends to form ion pairs of $[\text{C}_4\text{mim}]_{\text{org}}^+[\text{Dye}]_{\text{org}}^-$ that comprise part of the IL phase but according to NMR spectra, the structure is not altered so the IL can be recovered after several uses. In both cases, though, the PF_6^- is lost to the aqueous phase and would be introduced to the environment barring dedicated recovery steps (the remaining pair after combination would be $[\text{Dye}]_{\text{aq}}^+[\text{PF}_6]_{\text{aq}}^-$). This is the very opposite of “green” chemistry and needs to be addressed before this methodology can be considered viable.

In 2010, Fan *et al.* investigated the extraction of various azo dyes into C_4mimPF_6 , C_6mimPF_6 , C_8mimPF_6 , C_6mimBF_4 , and C_8mimBF_4 . The dyes included neutral 1-(phenylazo)-2-naphthol and 4-(nitrophenylazo) resorcinol, in addition to the cationic dyes 1-(2-pyridylazo)-2-naphthol, 4-(2-pyridylazo) resorcinol, and Methyl Red. They observed cation exchange, which involved the transfer of the cationic dye into the IL phase and the concomitant movement of the imidazolium cation into the aqueous phase. As long as the alkyl chain is sufficiently short, the cation lost to the aqueous phase may not be very toxic. Nonetheless, cation loss would affect the process economics. The

researchers also found higher D_{dye} values with the tetrafluoroborate ion than for the hexafluorophosphate ion, which was attributed to the greater hydrogen bonding ability of the former and the formation of hydrogen bonds between the dye and the IL. Finally, all but one dye was recovered (1-(phenylazo)-2-naphthol) [1.24].

It is clear from these studies that additional work is required: (a) to define the characteristics of an IL that leads to high extraction efficiency and facile recovery, (b) to elucidate the mechanism(s) by which dye molecules are extracted into an IL, and (c) to understand the seemingly contradicting results obtained by various investigations. With this in mind, a systematic study of the influence of IL cation hydrophobicity, IL anion properties, and dye characteristics on dye partitioning between a series of *N,N*-dialkylimidazolium-based ILs and water has been undertaken. Specifically, six different dyes were used to test the performance as extraction solvents of a series of ILs. These include three anionic dyes (Thymol Blue, Methyl Orange, and Orange G) and three cationic dyes (Methylene Blue, Safranin O, and Methyl Violet). These were chosen because they are representative of the two major families of commercial dyes, are stable in an array of media, have well-known structures, and are easy to handle.

1.5 Characteristics of Selected Dyes

. Thymol Blue is often used as a pH indicator. It is red below the first pK_a (1.7), yellow at pH values between 1.7 and its second pK_a (8.9), and Blue above pH 8.9. Methyl Orange is also used in acid-base titrations, but unlike Thymol Blue, it has only one pK_a (3.47). The dye is red at pH values below this pK_a and orange above it. Orange G is usually used in biological stains and gel electrophoresis. It is orange below a pH of 9 and red above it.

Methylene Blue is used frequently in biological stains and occasionally as a redox indicator. It has also found uses in the health care industry as a potential cure for malaria and certain cancers when combined with other drugs (such as indole-3-acetic acid). It maintains a consistent blue color regardless of pH, although it is insoluble at high pH values (above 10). Safranin O is also used in biological stains and in redox reactions; it maintains a dark pink/red color at all pH levels. The family of Methyl Violet dyes has been used as purple dye in the textile industry and in biological stains. It is generally yellow in very acidic solutions and dark purple above a pH of 1.6. Methyl Violet comprises a family of similar structures and in this particular work, structure 2B was used.

1.6 References

- 1.1 Pang, Y.L., and Abdullah, A.Z. "Current status of textile industry wastewater management and research progress in Malaysia: A review". *Clean Soil, Air, Water*, **2013**, 00 (0), 1-14.
- 1.2 Bokare, A.D., Chikate, R.C., Rode, C.V., and Paknikar, K.M. "Iron-nickel bimetallic nanoparticles for reductive degradation of azo dye Orange G in aqueous solution". *Applied Catalysis B: Environmental*, **2008**, 79, 270-278.
- 1.3 Bhat, R.V., and Mathur, P. "Changing scenario of food colours in India". *Current Science*, **1998**, 74 (3), 198-202.
- 1.4 Wang, Z., Xue, M., Huang, K., and Liu, Z. "Textile dyeing wastewater treatment". *Advances in Treating Textile Effluent*. Professor R. Hauser, Ed. InTech, <http://www.intechopen.com>, **2011**, 91-116.
- 1.5 Sharma, K.P., Sharma, K., Kumar, S., Sharma, S., Grover, R., Soni, P., Bhardwaj, S.M., Chaturvedi, R.K., and Sharma, S. "Response of selected aquatic macrophytes towards textile dye wastewaters". *Indian Journal of Biotechnology*, **2005**, 4, 538-545.
- 1.6 Kipcak, E., and Akgun, M. "In situ gas fuel production during the treatment of textile wastewater at supercritical conditions". *Water Science & Technology*, **2013**, 67.5, 1058-1067.

- 1.7 Pandit, P., and Basu, S. "Removal of ionic dyes from water by solvent extraction using reverse micelles". *Environmental Science & Technology*, **2004**, *38* (8), 2435-2442.
- 1.8 Muthuraman, G., and Teng, T.T. "Solvent extraction of methyl Violet with salicylic acid from aqueous acidic solutions". *Desalination*, **2010**, *263*, 113-117.
- 1.9 Mahmoud, A.S., Ghaly, A.E., and Brooks, M.S. "Removal of dye from textile wastewater using plant oils under different pH and temperature conditions". *American Journal of Environmental Sciences*, **2007**, *3* (4), 205-218.
- 1.10 Greaves, T.L., and Drummond, C.J. "Protic ionic liquids: Properties and applications". *Chemical Review*, **2008**, *108*, 206-237.
- 1.11 Huddleston, J.G., Willauer, H.D., Swatoski, R.P., Visser, A.E., and Rogers, R.D. "Room temperature ionic liquids as novel media for 'clean' liquid-liquid extraction". *Chem. Commun.*, **1998**, 1765-1766.
- 1.12 Zhang, S., Sun, N., He, X., Lu, X., and Zhang, X. "Physical properties of ionic liquids: Database and evaluation". *Journal of Physical Chemical Reference Data*, **2006**, *35* (4), 1475-1517.
- 1.13 Holbrey, J.D. and Seddon, K.R. "Ionic liquids". *Clean Products and Processes 1*, **1999**, 223- 236.
- 1.14 Stasiewicz, M., Mulkiewicz, E., Tomczak-Wandzel, R., Kumirska, J., Siedlecka, E.M., Golebiowski, M., Gajdus, J., Czerwicka, M., and Stepnowski, P. "Assessing toxicity and biodegradation of novel, environmentally benign ionic liquids (1-alkoxymethyl-3-hydroxypyridinium chloride saccharinate and acesulfamates) on cellular and molecular level". *Ecotoxicology and Environmental Safety*, **2008**, *71*, 157-165.
- 1.15 Peric, B., Marti, E., Sierra, J., Cruanas, R., Iglesias, M., and Garau, M.A. "Terrestrial ecotoxicity of short aliphatic protic ionic liquids". *Environmental Toxicology and Chemistry*, **2011**, *30* (12), 2802-2809.
- 1.16 Cyjetko, M., Radosevic, K., Tomica, A., Slivac, I., Vorkapic-Furac, J., and Gaurina Sreck, V. "Cytotoxic effects of imidazolium ionic liquids on fish and human cell lines". *Arh Hig Rada Toksikol*, **2012**, *63*, 15-20.
- 1.17 Viboud, S., Papaiconomou, N., Cortesi, A., Chatel, G., Draye, M., and Fontvieille, D. "Correlating the structure and composition of ionic liquids with their toxicity on *Vibrio fischeri*: a systematic study". *Journal of Hazardous Materials*, **2012**, *215-216*, 40-48.

- 1.18 Rydberg, J. *Solvation Extraction Principles and Practice, Revised and Expanded*. CRC Press: Boca Raton, FL. **2004**.
- 1.19 Visser, A.E., Swatloski, R.P., and Rogers, R.D. "pH-Dependent partitioning in room temperature ionic liquids". *Green Chemistry*, **2000**, 1-4.
- 1.20 Vijayaraghavan, R., Vedaraman, N., Surianarayanan, M., and MacFarlane, D.R. "Extraction and recovery of azo dyes in an ionic liquid". *Talanta*, **2006**, *69*, 1059-1062.
- 1.21 Ali, M., Sarkar, A., Pandey, M.D., and Pandey, S. "Efficient precipitation of dyes from dilute aqueous solutions of ionic liquids". *Analytical Sciences*, **2006**, *22*, 1051-1053.
- 1.22 Pei, Y.C., Wang, J.J., Xuan, X.P., Fan, J., and Fan, M. "Factors affecting ionic liquids based removal of anionic dyes from water". *Environmental Science & Technology*, **2007**, *41 (14)*, 5090-5095.
- 1.23 Li, C., and Xin, B. "Extraction and mechanisms of acid dyes into a room temperature ionic liquid". *2nd International Conference on Bioinformatics & Biomedical Engineering*, **2008**, 3519-3522.
- 1.24 Fan, J., Fan, Y., Zhang, S., and Wang, J. "Extraction of azo dyes from aqueous solutions with room temperature ionic liquids". *Separation Science and Technology*, **2011**, *46*, 1172-1177.

CHAPTER 2: DYE DISTRIBUTION IN OCTANOL-WATER SYSTEMS

2.1 Introduction

While it is generally accepted that in terms of fugative emissions ionic liquids are more environmentally-friendly than traditional solvents, the toxicity and effects on aquatic environments of most ILs remain incompletely understood. The research that has been conducted indicates that both the cationic and anionic components can be harmful to aquatic organisms such as bacteria, algae, freshwater snails, and catfish, among others [2.1-2.2]. It is possible that many ILs will prove sufficiently toxic as to defeat the purpose of using them to remove dyestuffs from water. It is therefore critical to understand how dyes will act in IL systems. One way to begin studying this is to examine the octanol-water partitioning coefficient (D_{ow}) and $\log D$, of a given dye. Huddleston *et al.* have noted that an IL system (*i.e.*, 1-methyl-3-butylimidazolium hexafluorophosphate) yields partition coefficients for a number of solutes that correlate well with those found in an octanol-water system [2.3]. Therefore, this value, which can be used to describe a dye as hydrophobic or hydrophilic, could potentially also be used to predict how the dye will behave in the ILs of interest here.

In this portion of the work, the D_{ow} of four dyes was determined using the “slow-stir” method [2.4] in which a glass vessel was filled with equal volumes of dye-saturated water and dye-saturated octanol and stirred slowly and continuously until equilibrium was reached. To reduce or eliminate the possibility of cross-contamination between phases, a length of tubing was added so that the denser water phase could be sampled

independently of the octanol layer. Figure 2.1 provides a side-view of the sampling vessel [2.4].

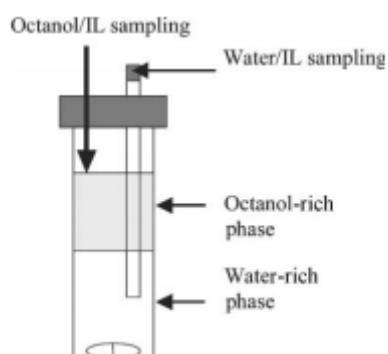


Figure 2.1 Apparatus used for octanol-water systems.

2.2 Experimental

2.2.1 Materials

The 1-octanol was obtained from Alfa Aesar (Heysham, England) and had a purity of 99% (v/v). The water with which the octanol was equilibrated was obtained from an Easypure II system and had a resistivity of 18.2 M Ω . Three of the dyes (methyl Orange, Methylene Blue, and Safranin O) were purchased from Sigma-Aldrich (Milwaukee, WI), while the fourth (Methyl Violet) was obtained from Acros Organics (Fair Lawn, NJ). Only four dyes were considered here for reasons that will be outlined in a later section of this report. Twenty-five milliliters of a 1 mM solution of each dye were prepared by dissolving the appropriate mass of solid in either water or 1-octanol, as appropriate. From these stock solutions, dye standards of varying concentrations (*ca.* 0.002-0.025 mM) in both octanol and water were made for use in UV-visible spectrophotometric measurements. The concentrations were chosen to exhibit a range of absorbances between 0.000 and 1.000.

2.2.2 Instrumentation

Measurements of dye concentration were made using UV-visible spectrophotometry (Shimadzu UV-2450 Spectrophotometer). This instrument relies on Beer's Law (Eqn. 2-1) which states that the absorbance of a sample is directly proportional to the concentration of light-absorbing molecules [2.5]. "A" represents absorbance, ϵ represents molar absorptivity in $M^{-1}cm^{-1}$, b represents the pathlength in cm, and c represents the concentration in M.

$$A = \epsilon bc \quad (2-1)$$

Quartz cuvettes with a path length of 1.0 cm were used. All samples were measured against a reference cell that contained either water or octanol, depending on the diluent used for the sample. The spectrophotometer can be represented by a schematic such as the one depicted in Figure 2.2, and specific operating conditions are listed in Table 2.1. All measurements were conducted at the wavelength of maximum absorbance for each dye in each diluent (Table 2.2), which was determined by obtaining a spectrum of the dye solution over the range specified in Table 2.1.

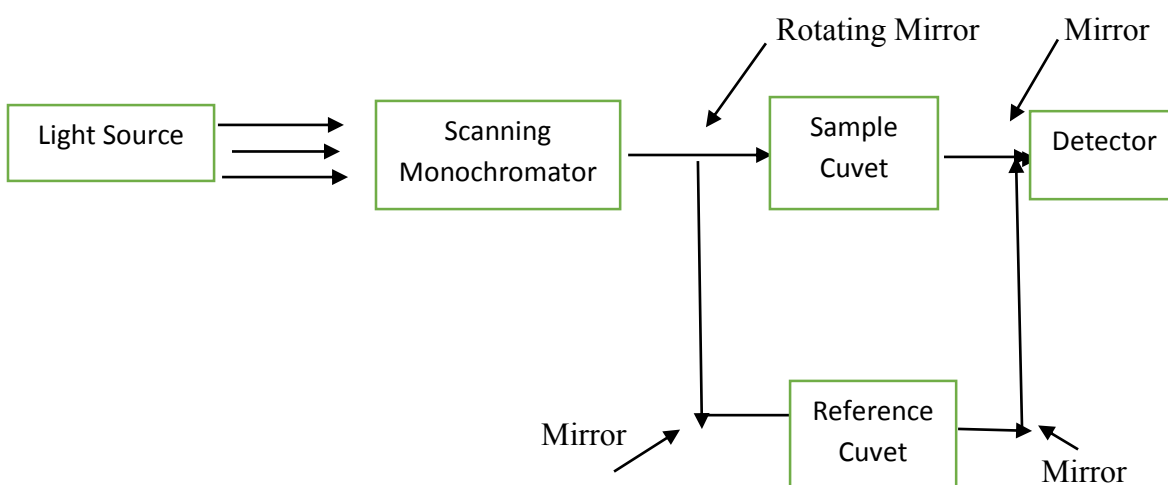


Figure 2.2 Spectrophotometer Schematic (Adapted from 2.5)

Table 2.1
UV-Visible Spectrophotometer Operating Conditions

Range of Wavelengths	900-190 nm
Scan Rate	210 nm/min
Sampling Interval	1.0 nm
Slit Width	2.0 nm
Number of Measurements	3
Time Delay	10 seconds
Light Source*	50W Halogen and Deuterium
Photometric Accuracy*	± 0.002 Abs between 0-0.5 ± 0.004 Abs between 0.5-1.0
Drift*	< 0.004 Abs/hour

*[2.6]

Table 2.2
Wavelength of Maximum Absorbance for Dyes

Dye	λ_{\max} in Water (nm)	λ_{\max} in Octanol (nm)
Methyl Orange	471	417
Methylene Blue	664	660
Safranin O	520	539
Methyl Violet	577	583

2.2.3 Procedure

A 15-mL aliquot of an aqueous dye solution was placed into the equilibration vessel (depicted in Figure 2.1), followed by thin plastic tubing (Hamilton). After the tubing was secured in the aqueous layer, a 15 mL sample of the same dye in octanol was added. The tubing was then pulled through a pierced rubber septum and secured with a small plastic cover. Using a micro stir bar, each octanol-water dye system was continuously stirred for a period of three to four months. Samples were withdrawn periodically from each phase for analysis by UV-visible spectrophotometry.

Specifically, sampling was accomplished using a 250 or 500 μ L Hamilton glass syringe. The water layer was sampled through the tubing while the octanol layer was

sampled by piercing the rubber septum with the syringe needle. The volume removed varied depending upon the color saturation and, as time passed, the volume that could be removed without disturbing the tubing. Calibration curves for each dye in each phase were constructed using standard solutions that ranged in concentration from 0.002 to 0.025 mM. Dilutions were made as necessary to ensure that all measured absorbances fell between 0.000 and 1.000 and fit within the standard calibration curves. Sampling was completed either when the volumes of the respective phases became too small or when the concentrations in both phases had not shown any significant change over the preceding 30 days. The distribution ratio for a given dye in an octanol-water system, or D_{ow} , was calculated by dividing the concentration of dye in the octanol layer by the concentration in the aqueous layer. A D_{ow} value was calculated for each sampling point, and graphs of D_{ow} over time were constructed. All systems were considered to be in equilibrium beyond a point of 104 to 133 days of constant stirring.

2.3 Results

Figure 2.3 shows the D_{ow} obtained for Methyl Orange. Methylene Blue data are provided in Figure 2.4. Safranin O data are shown in Figure 2.5. Finally, Methyl Violet data are presented in Figure 2.6. Error bars are not included because only one sample for each phase was acquired at each sampling time. Table 2.3 shows the D_{ow} and $\log D$ for each dye at the equilibrium point.

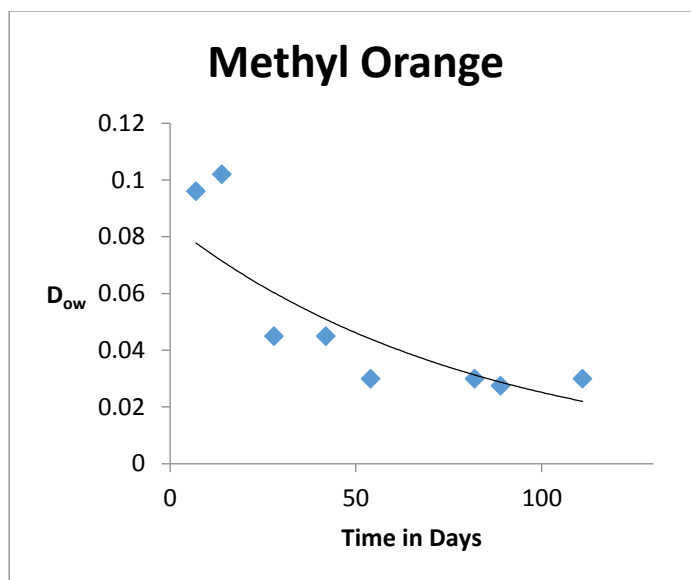


Figure 2.3 Distribution ratio of Methyl Orange in an octanol-water system over time.

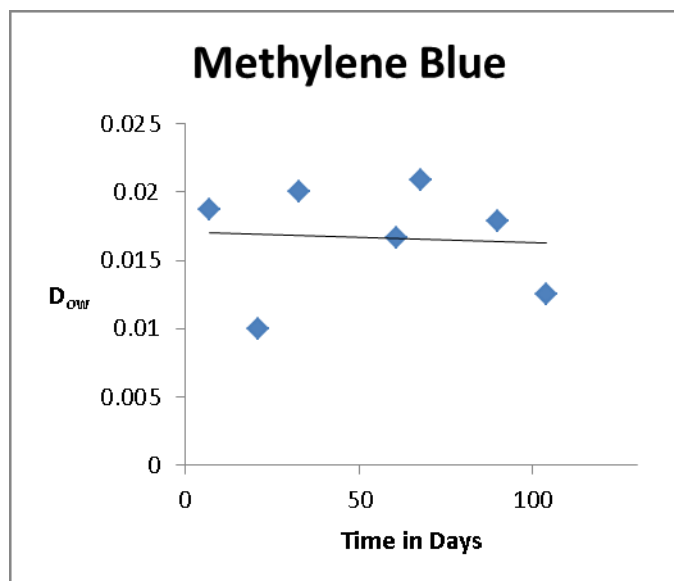


Figure 2.4 Distribution ratio of Methylene Blue in an octanol-water system over time

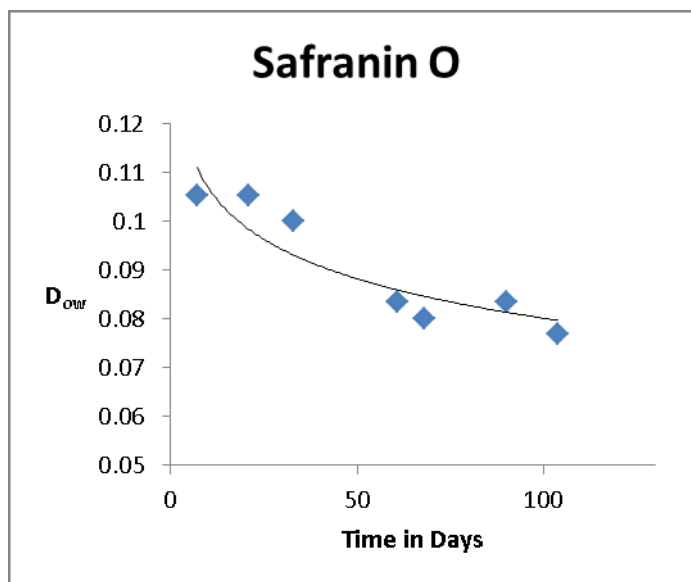


Figure 2.5 Distribution ratio of Safranin O in an octanol-water system over time

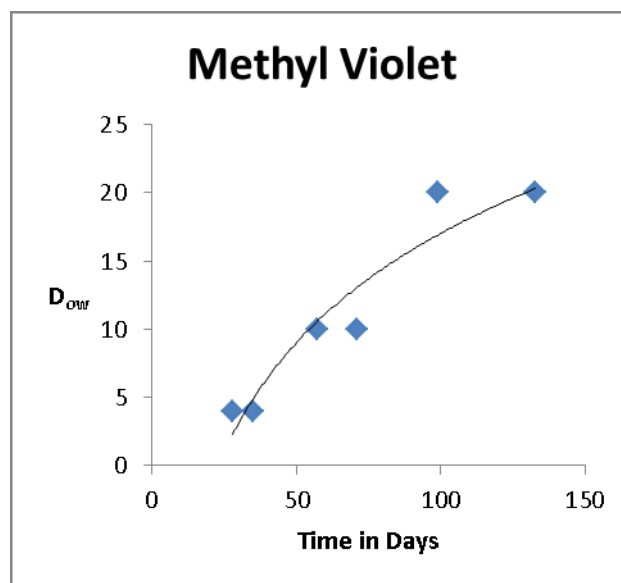


Figure 2.6 Distribution ratio of Methyl Violet in an octanol-water system over time.

Table 2.3
 D_{ow} and log D at Equilibrium Point

Dye	D_{ow}	Log D
Methyl Orange	0.030	-1.522
Methylene Blue	0.013	-1.886
Safranin O	0.077	-1.114
Methyl Violet	20.00	1.301

2.4 Discussion

The objective of this portion of the work was to observe the behavior of dyes in a “conventional” solvent system comprising only octanol and water. Originally, six dyes were to be examined in this study, but two of them (Thymol Blue and Orange G) were eventually abandoned due to various circumstances that made their determination difficult or impossible. Thymol Blue, for example, yielded aqueous phase absorbance values too low to be measured reliably, thus preventing the calculation of a D_{ow} value. Orange G did not readily dissolve in octanol, thus rendering any study of its partitioning impractical. Determination of the partitioning of these dyes in an octanol-water system awaits the development of alternative methodology.

Regarding the systems for which reliable measurements were possible, it can be seen that Methyl Orange ($D_{ow} = 0.030$), Methylene Blue ($D_{ow} = 0.013$), and Safranin O ($D_{ow} = 0.077$) favor the aqueous phase, while Methyl Violet ($D_{ow} = 20.00$) heavily favors the octanol phase. Methylene Blue was the most hydrophilic, followed by Safranin O and Methyl Orange. It might reasonably be anticipated that these trends also hold for dye partitioning between water and various ionic liquids, with dyes such as methyl Orange favoring the aqueous phase and Methyl Violet favoring the IL phase.

2.5 References

- 2.1 Viboud, S., Papaiconomou, N., Cortesi, A., Chatel, G., Draye, M., and Fontvieille, D. “Correlating the structure and composition of ionic liquids with their toxicity on *Vibrio fischeri*: a systematic study”. *Journal of Hazardous Materials*, **2012**, 215-216, 40-48.
- 2.2 Cvjetko, M., Radosevic, K., Tomica, A., Slivac, I., Vorkapic-Furac, J., and Gaurina Sreck, V. “Cytotoxic effects of imidazolium ionic liquids on fish and human cell lines”. *Arh Hig Rada Toksikol*, **2012**, 63, 15-20.

2.3 Huddleston, J.G., Willauer, H.D., Swatloski, R.P., Visser, A. E., and Rogers, R.D. "Room temperature ionic liquids as novel media for 'clean' liquid-liquid extraction". *Chemical Communications*, **1998**, 1765-1766.

2.4 Ropel, L., Belveze, L.S., Aki, S.N.V.K., Stadtherr, M.A., and Brennecke, J.F. "Octanol-water partition coefficients of imidazolium-based ionic liquids". *Green Chemistry*, **2005**, 7, 83-90.

2.5 Harris, D.C. *Exploring Chemical Analysis*. **2013**, 5th edition. W.H. Freeman and Company: New York City, NY.

2.6 Shimadzu Instruction Manual. *UV-2450/2550 User's System Guide*, **2006**, Shimadzu Corporation: Kyoto, Japan.

CHAPTER 3:

DEVELOPMENT OF AN EXTRACTION PROCEDURE: DYE DISTRIBUTION IN 1-METHYL-3-OCTYLIMIDAZOLIUM HEXAFLUOROPHOSPHATE ($C_8mim^+PF_6^-$)—WATER SYSTEMS

3.1 Introduction

As the next step in the development of a procedure for evaluating dye partitioning in IL-water systems, the extraction of Thymol Blue from water into 1-octyl-3-methylimidazolium hexafluorophosphate (C_8mimPF_6), a system previously studied by Visser *et al.* [3.1], was examined. The extraction of Thymol Blue was measured at five different pH values (*i.e.*, 1.5, 2, 4, 7, and 12) and the distribution ratio was calculated for each pH. A graph of the distribution ratio of the dye versus pH was then constructed and compared to prior results obtained using a similar procedure [3.1].

3.2 Experimental

3.2.1 Materials

Thymol Blue (12.3 mg; Sigma-Aldrich, Milwaukee, WI), was weighed into a series of 25-mL volumetric flasks. Each portion was dissolved and diluted to the mark with the appropriate diluent to achieve a concentration of 1 mM. Acidic solutions (*i.e.*, pH 1.5, 2, and 4) were prepared by dilution of concentrated sulfuric acid (18.16 M; Sigma-Aldrich, St. Louis, MO), while other solutions were made via the dilution of concentrated sodium hydroxide (19.9 M; Fluka/Sigma, St. Louis, MO). The pH of all solutions was measured using an Orion 720A+ pH meter (Thermo Scientific) and adjusted to the appropriate pH by the addition of acid or base as needed.

The ionic liquid, C_8mimPF_6 , was prepared in a two-step process. In the first step, 1-octyl-3-methylimidazolium bromide (C_8mimBr) was synthesized by combining 1-

methylimidazole (Acros Organics, Fair Lawn, NJ) with 5% (v/v) molar excess of bromooctane (Acros Organics, Fair Lawn, NJ) in a glass microwave vial. This mixture was then placed in a CEM Discovery (Matthews, NC) microwave apparatus and heated for 8 minutes at a temperature of 110°C and a power setting of 240 W, as suggested by Deetlefs and Seddon (2003) [3.2]. Six vials were microwaved simultaneously and the combined product was subjected to multiple (≥ 3) washes with ethyl acetate to remove excess bromooctane. The washed product was then rotovapped (Buchi Rotovapor RII, Flawil, Switzerland) to remove the ethyl acetate. The structure of the IL was confirmed *via* proton NMR using deuterated chloroform (CDCl_3 , Alfa Aesar, Ward Hill, MA) as the diluent.

In the second step, a known quantity of C_8mimBr was reacted with a 5% (v/v) molar excess of potassium hexafluorophosphate (Acros Organics, Fair Lawn, NJ). Specifically, the C_8mimBr was dissolved in ultra-pure water and stirred in a round-bottom flask, which was positioned in a large beaker and surrounded by ice. The KPF_6 , also dissolved in ultra-pure water, was slowly added to the same flask while stirring was maintained. The mixture was stirred for 12 to 24 hours, during which time $\text{C}_8\text{mim}^+\text{PF}_6^-$ formed as a separate layer. This layer was removed, then washed with water to remove excess KPF_6 . The IL was then rotovapped to remove any water, and its structure was confirmed *via* proton-NMR using deuterated dimethyl sulfoxide (DMSO, Acros Organics, Fair Lawn, NJ) as the diluent [3.3]. The percent yields ranged from 70 to 80%.

3.2.2 Instrumentation

All pH measurements were made using an Orion model 720A+ (Thermo Scientific). The UV-visible spectrometer used was that previously mentioned (section

2.2.2). Quartz cuvettes having a path length of 1 cm were used. Absorbances were measured at the wavelength of maximum absorption of the dye at each pH (Table 3.1). Proton NMR spectra were obtained on a Bruker DPX 300 using a 5-mm broadband probe. Operating conditions for the NMR, such as the gradient shimming values and receiver gain, varied with each measurement.

3.2.3 Procedures

For quantification of the dyes, a series of calibration standards were prepared at each pH at concentrations ranging from 0.002 to 0.2 mM, which yielded an absorbance between 0 and 1.

Table 3.1
Wavelengths of Maximum Absorbance

pH	λ_{max} (in nm)
1.50	544
2.00	423
4.00	430
7.00	434
12.00	596

One milliliter aliquots of C_8mimPF_6 were pipetted into a series of fifteen culture tubes (each pH level was run in triplicate to decrease error). To each was added ~ 1 mL of an appropriate pH solution. The tubes were sealed and gently vortexed for approximately 30 seconds. Each mixture was then centrifuged for 3 minutes, following which the aqueous layer was removed and discarded. This process was repeated a second time to condition the IL. Next, a 3 mL aliquot of an aqueous solution (1 mM) of Thymol Blue at the appropriate pH was added to the culture tubes. The vortexing and centrifugation were then repeated. The mixtures were allowed to stand undisturbed for

ten minutes to ensure sufficient time for distribution of the dye. The aqueous layer was then removed and analyzed using the UV-visible spectrometer. In the study of Visser *et al.*, a 1:1 phase volume ratio was used, but the minimum volume required for the UV-vis spectrometer is ca. 2.5 mL. Therefore, a volume of 3 mL was chosen so that there would be sufficient sample even without dilution. In fact, samples were diluted only if the absorbance exceeded 1.

The distribution ratio was calculated in a different manner than indicated in Eqn. 1-1. That is, in these experiments, the dye concentration in the ionic liquid layer could not be measured directly due to the fact that ILs have UV-visible absorbance bands that overlap those of the dyes. Therefore the amount of dye in the IL layer was determined by difference (*i.e.*, the original aqueous phase concentration (1 mM) less that remaining after equilibration). Thus, D_{dye} was calculated as per Eqn. 2-2 (below). Note that the multiplication by 3 accounts for the 3:1 phase-to-volume ratio.

$$D = \frac{[1\text{mM}] - [\text{concentration of aqueous layer}]}{[\text{concentration of aqueous layer}]} \times 3 \quad (3-2)$$

3.3 Results

Visser *et al.* found distribution ratios for Thymol Blue between 100 and 1000, with the highest values at acidic and neutral pH. There was a marked drop (down to about 1) in D_{dye} , however, at basic pH values. The distribution ratios determined here showed much the same trend. Figure 3.2 summarizes the values observed at each pH (all represent an average of three trials).

As can be seen, the results correspond reasonably well to those of Visser *et al.* That is, the distribution ratio for pH 1.5 is slightly higher than that at pH 2 or 4, while the value at a pH 7 is higher still. Above a pH of 7, the D_{dye} values decline precipitously,

falling to *ca.* one or less at pH 12, thus indicating that the neutral form of the dye is preferentially extracted into the IL phase, while the anionic form favors the aqueous phase.

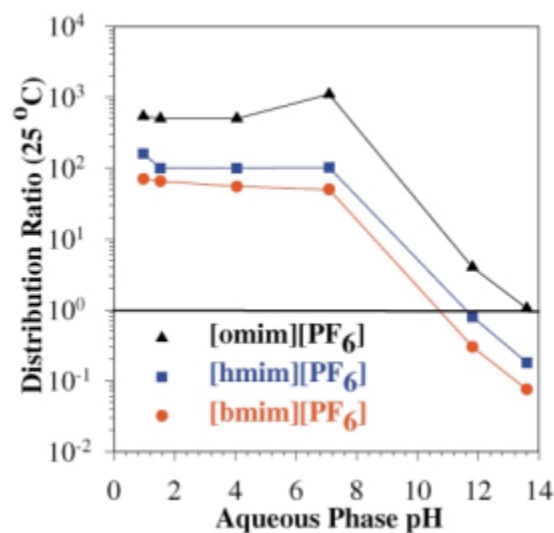


Figure 3.1 Distribution ratios vs. pH for Thymol Blue from Visser et al.

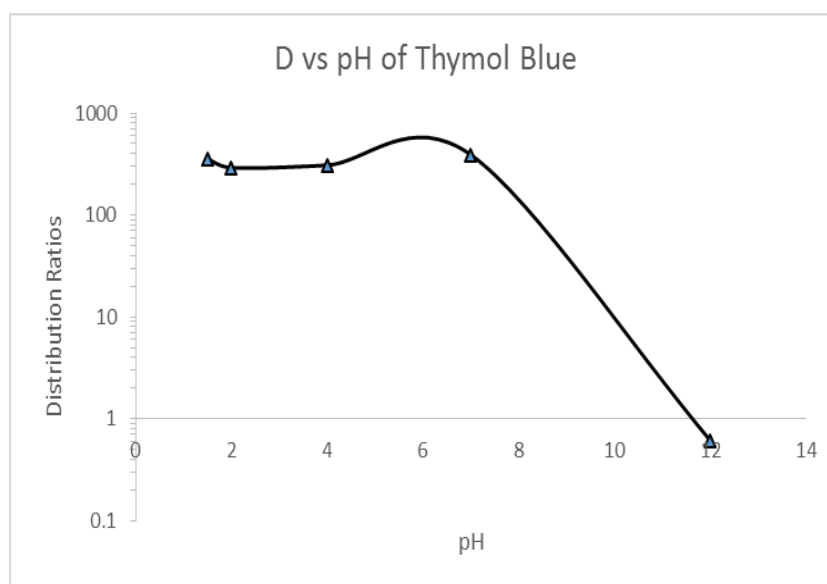


Figure 3.2 Distribution ratios vs. pH of Thymol Blue for [C₈mim][PF₆]

3.4 Conclusions

The objective of this experiment was to verify that the extraction procedure and method of measuring dye concentrations to be employed provides satisfactory results. To

this end, Thymol Blue extraction into an ionic liquid (C_8mimPF_6) previously examined by Visser *et al.* was studied. The results obtained track closely those obtained by previous investigators in that the distribution ratio (*i.e.*, the extraction efficiency) was found to significantly decline at basic pH values. These results indicate that the procedure to be used here is entirely appropriate.

3.5 References

- 3.1 Visser, A.E., Swatloski, R.P., and Rogers, R.D. "pH-Dependent partitioning in room temperature ionic liquids". *Green Chemistry*, **2000**, 1-4.
- 3.2 Deetlefs, M., and Seddon, K.R. "Improved preparations of ionic liquids using microwave irradiation". *Green Chemistry*, **2003**, 5, 181-186.
- 3.3 Pei, Y., Liu, J., Yan, Z., Li, Z., Fan, J., and Wang, J. "Association of ionic liquids with cationic dyes in aqueous solution: A thermodynamic study". *Journal of Chemical Thermodynamics*, **2012**, 47, 223-227.

CHAPTER 4: DYE EXTRACTION INTO IONIC LIQUIDS

4.1 Introduction

Having demonstrated the viability of the approach to be employed in measuring dye partitioning on a “known” dye sample, the next step was to examine the extraction of the various dyes of interest into a series of ionic liquids. Three imidazolium-based cations differing in the lengths of the attached alkyl chains (six, eight, or ten carbons), were used. Two different anions, hexafluorophosphate (PF_6^-) and *bis* [(trifluoromethyl) sulfonyl] imide (Tf_2N^-), were paired with each cation. Thus six ionic liquids were evaluated in all. Six dyes, three anionic (*i.e.*, Thymol Blue, Methyl Orange, and Orange G) and three cationic (*i.e.*, Methylene Blue, Safranin O, and Methyl Violet 2B), were also examined, with the objective of elucidating the characteristics of both the IL and the dye that determine the extent to which a given dye is extracted.

4.2 Experimental

4.2.1 Materials

Thymol Blue, Methyl Orange, Orange G, Methylene Blue, and Safranin O were obtained from Sigma-Aldrich (Milwaukee, WI). Methyl Violet 2B was obtained from Acros Organics (Fair Lawn, NJ). Dye solutions were prepared in a manner identical to that described in section 3.2.1. The octanol used was from Alfa Aesar (Ward Hill, MA) and had a purity of 99% (v/v).

The ionic liquid C_8mimPF_6 was prepared using the procedure outlined in Section 3.2.1. The ionic liquids C_6mimBr and $\text{C}_{10}\text{mimBr}$ were prepared using 1-methylimidazole (Acros Organics, Fair Lawn, NJ) and a 5% (v/v) excess of 1-bromohexane (Acros Organics, Fair Lawn, NJ) or 1-bromodecane (Sigma-Aldrich, St. Louis, MO),

respectively. In both cases, six reaction tubes were irradiated in the microwave using the following parameters: microwave power of 240 watts, temperature of 80°C and time of 8 minutes for C₆mimBr; microwave power of 240 watts, temperature of 120°C and time of 10 minutes for C₁₀mimBr, as suggested by Deetlefs & Seddon [4.1]. Final structures were confirmed *via* proton-NMR using deuterated chloroform (Alfa Aesar, Ward Hill, MA) as the diluent. The metathesis procedures for C₆mimPF₆ and C₁₀mimPF₆ were essentially identical to that described for C₈mimPF₆. The structure of each ionic liquid was confirmed *via* proton-NMR using DMSO (Acros Organics, Fair Lawn, NJ) as the solvent for the ILs comprised of the PF₆⁻ anion and using CDCl₃ for the ILs comprised of the Tf₂N⁻ anion.

The ionic liquids C₆mimTf₂N, C₈mimTf₂N, and C₁₀mimTf₂N were prepared from the corresponding bromides (*i.e.*, C₆mimBr, C₈mimBr, and C₁₀mimBr, respectively). The metathesis step involved the reaction between a solution of lithium *bis* [(trifluoromethyl) sulfonyl] imide (LiTf₂N, Wako Chemicals, Osaka, Japan) dissolved in ultra-pure water and the appropriate precursor, also dissolved in water. The mixture was allowed to stir for 24 hours, during which time the IL formed as a separate phase. After multiple (4-5) water washes, the IL was dried by rotary evaporation and heating (up to 80°C). The IL structures were confirmed using proton-NMR with deuterated chloroform as the diluent. The yields were generally satisfactory, typically between 70 and 80%.

. The solutions for dye stripping included 0.1 M sodium hydroxide (Fluka/Sigma, St. Louis, MO, 19.9 M), 1.0 M hydrochloric acid (Fisher Chemicals, Pittsburgh, PA), and 50% (v/v) ethanol/water (Koptec, King of Prussia, PA).

4.2.2 Instrumentation

The instrumentation described in Section 2.2 of Chapter 3 was used in this experiment.

4.2.3 Procedures

The procedures followed were similar to those described in Section 3.2.3, but the volumes of IL and 1-octanol used were reduced to only 0.5 mL. All extractions were again performed in triplicate and the same preconditioning steps applied. Three milliliters of dye solution were added as before, thus changing the phase ratio to a factor of 6 (3 mL of dye / 0.5 mL of ionic liquid). For each dye, the absorbance was measured at its isosbestic point (Table 4.1).

$$D = \frac{[1 \text{ mM}] - [\text{concentration of aqueous layer}]}{[\text{concentration of aqueous layer}]} \times 6 \quad (4-1)$$

Table 4.1
Isosbestic Points

Dye	Isosbestic Point (in nm)
Thymol Blue	490
Methyl Orange	504
Orange G	493
Methylene Blue	660
Safranin O	520
Methyl Violet	585

Once the measured absorbance values had been converted to concentration *via* the calibration curves, the distribution ratio for each dye at each pH was calculated from Eqn. 4-1. A typical calibration curve, here for Methylene Blue, is shown in Figure 4.1. Calibration curves for each dye ranged as follows: for Thymol Blue, from 0.002 to 0.2 mM, for Methyl Orange, from 0.005 to 0.1 mM, for Orange G, from 0.005 to 0.1 mM, for

Methylene Blue, from 0.001 to 0.015 mM, for Safranin O, from 0.002 to 0.025 mM, and for Methyl Violet, from 0.002 to 0.015 mM.

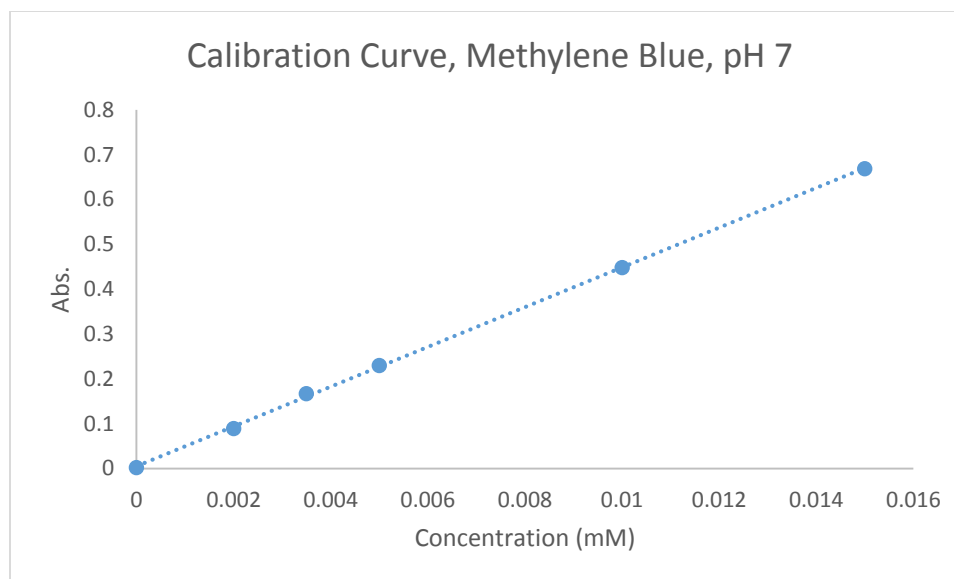
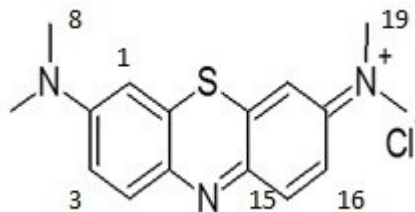


Figure 4.1 Calibration Curve for Methylene Blue at pH 7

4.3 Results

4.3.1 Methylene Blue Extraction

Given its structure (Figure 4.2), the cationic dye Methylene Blue (MB^+) (UV-visible spectrum at pH 7, Figure 4.3) was not expected to exhibit pH-dependent partitioning for any of the ILs considered. Indeed as can be seen from Figure 4.4, the dependence of D_{dye} on pH for a given IL is essentially flat. Over the entire pH range, in fact, MB^+ is extracted quite well by all the ionic liquids, with D values reaching nearly 3000 for C_6mimPF_6 (Figure 4.4). In contrast, 1-octanol failed to extract any measurable amount of dye. (Although this would seem to contradict prior work indicating that the partitioning of organic molecules into an ionic liquid is correlated with its octanol-water partition coefficient [4.2], this correlation apparently applies to the uncharged form of ionizable solutes.)



pKas at following carbons [4.3]:

C1	—32.6
C3	—33.7
C8	—37.2
C15	—34.0
C16	—36.9
C19	—26.2

Figure 4.2 Methylene Blue

Overall, ILs incorporating the relatively hydrophilic $C_6\text{mim}^+$ cation yielded higher values of D_{dye} than those incorporating cations with longer alkyl chains. In fact, D_{dye} was generally found to decline as the size (i.e., hydrophobicity) of the IL cation increased. This suggests that cation-exchange involving the exchange of the MB^+ cation for the cationic component of the IL is likely to be the predominant mode of partitioning of this dye into these ILs (Eqn. 4-2). This mode of extraction is reminiscent of the mechanism seen for the extraction of metal ions into ILs [4.4] by neutral extractants (e.g., crown ethers), in which a cationic metal-extractant complex is exchanged for the IL cation.



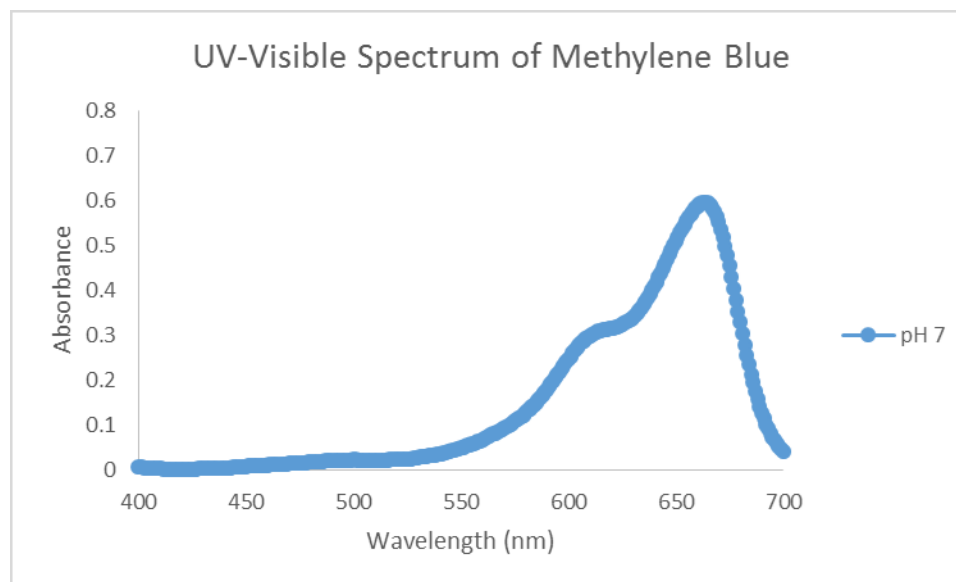


Figure 4.3 UV-Visible Spectrum of Methylene Blue

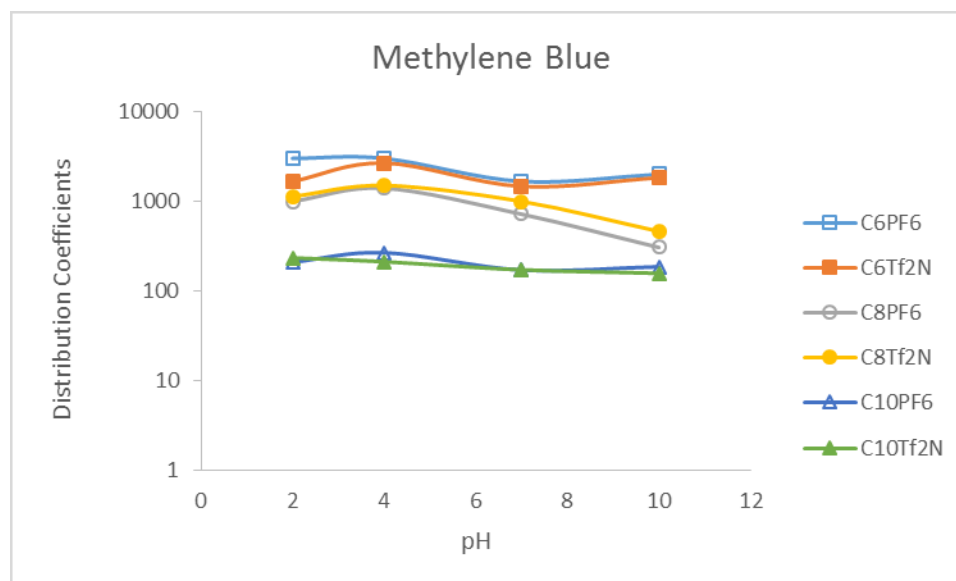
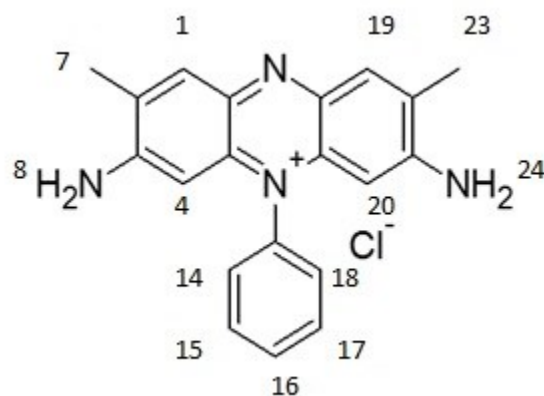


Figure 4.4 Distribution coefficient vs pH for Methylene Blue

4.3.2 Safranin O Extraction

The extraction of Safranin O (Figure 4.5; UV-visible spectrum, Figure 4.6) follows a trend similar to that of Methylene Blue, in particular, significant dye extraction into the ILs and negligible extraction into octanol (except at a pH of 12). Here too, more efficient extraction is observed for ILs incorporating smaller cations. For ILs

incorporating the PF_6^- anion, D_{dye} values ranging from 100 to nearly 1000 were observed, with best results being obtained for C_6mimPF_6 . ILs with the Tf_2N^- anion yielded slightly better results than their PF_6^- counterparts, with D_{dye} values reaching nearly 5000 and staying above 100. As was the case for PF_6^- , the IL incorporating the most hydrophilic cation ($\text{C}_6\text{mimTf}_2\text{N}$) provided the highest extraction efficiency. As with Methylene Blue, the D_{dye} values vary little with pH (Figure 4.7).



pKas at following atoms [4.3]:

- C1—36.9
- C4—35.7
- C7—29.0
- N8—12.3
- C14—35.5
- C15—36.1
- C16—36.9
- C17—36.1
- C18—35.5
- C19—33.2
- C20—34.4
- C23—35.2
- N24—25.0

Figure 4.5 Safranin O

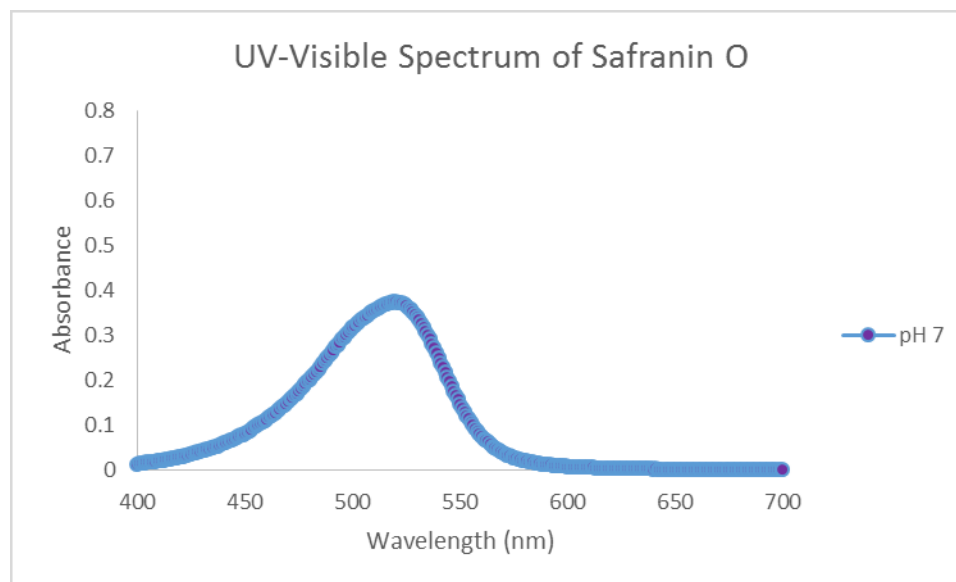


Figure 4.6 UV-Visible Spectrum of Safranin O

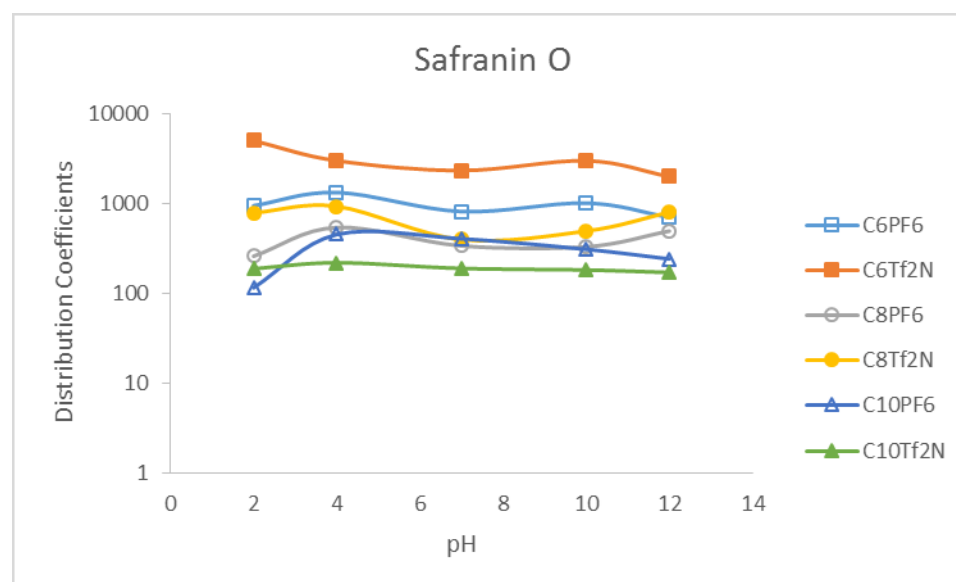


Figure 4.7 Distribution coefficient vs pH for Safranin O

The large values of D_{dye} , along with the increase in extraction that accompanies a decrease in IL cation hydrophobicity, suggest that cation exchange is again the predominant mode of extraction for the dye (Eqn. 4-3).



Also consistent with this mode of extraction is the fact that higher values of D_{dye} are observed for the more hydrophobic Tf_2N^- anion. That is, for any given IL cation, the more hydrophilic the IL anion, the greater the aqueous solubility of the IL, and thus the greater the concentration of C_nmim^+ in the aqueous phase. Obviously, higher concentrations of C_nmim^+ will suppress the cation exchange process (Eqn. 4-3), resulting in lower dye partitioning. In this respect then, Safranin O extraction mimics the extraction of charged metal complexes [4.4], as was the case for Methylene Blue.

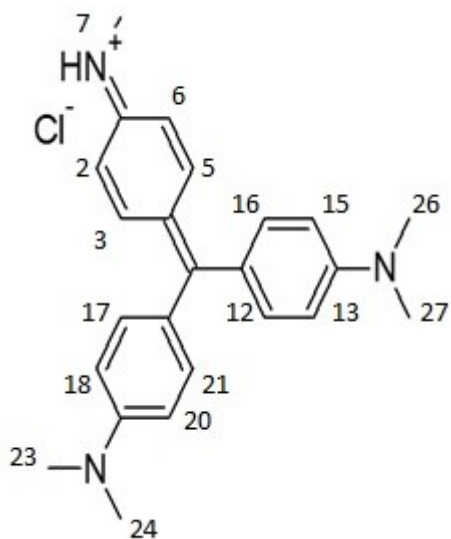
4.3.3 Methyl Violet Extraction

Unlike Methylene Blue and Safranin O, Methyl Violet is a protonated amine (Figure 4.8; UV-visible spectrum, Figure 4.9). Not unexpectedly then, MV partitioning is more sensitive to changes in the aqueous pH than is the distribution of the other two cationic dyes. Specifically, increasing pH, which would be accompanied by deprotonation of MVH^+ to yield the neutral dye, results in a decrease in D_{dye} (Figure 4.10). Like MB and SO, however, the D_{dye} values for MV increase with decreasing IL cation hydrophobicity ($\text{C}_{10}\text{mim} < \text{C}_8\text{mim} < \text{C}_6\text{mim}$), again consistent with cation exchange (Eqn. 4-4) as the predominant mode of dye partitioning.



As was the case for SO, for a given IL cation, the Tf_2N^- anion yielded consistently higher D_{dye} values than the corresponding PF_6^- ILs, again consistent with cation exchange as the major path for dye partitioning [4.4]. Overall, D_{dye} was poorest for extraction into $\text{C}_{10}\text{mimPF}_6$. In fact, in this system, D_{dye} was lower than that observed for either other dye.

Methyl Violet was the only cationic dye to be appreciably extracted into octanol, as can be seen in Figure 4.10, which depicts the pH dependence of D_{dye} (as with Methylene Blue, a pH of 12 was not used due to a lack of solubility). As can be seen, extraction into 1-octanol improves markedly as the pH rises. These results too are consistent with the existence of two forms of the dye, one charged and the other neutral, and the preferential partitioning of the latter form, as would be expected for a conventional organic solvent.



pKas at the following atoms [4.3]:

C2—36.3
 C3—35.4
 C5—35.4
 C6—36.3
 N7—24.8
 C12—35.3
 C13—36.1
 C15—36.1
 C16—35.3
 C17—37.4
 C18—38.3
 C20—38.3
 C21—37.4
 C23—26.2
 C24—26.2
 C26—37.2
 C27—37.2

4.8 Methyl Violet

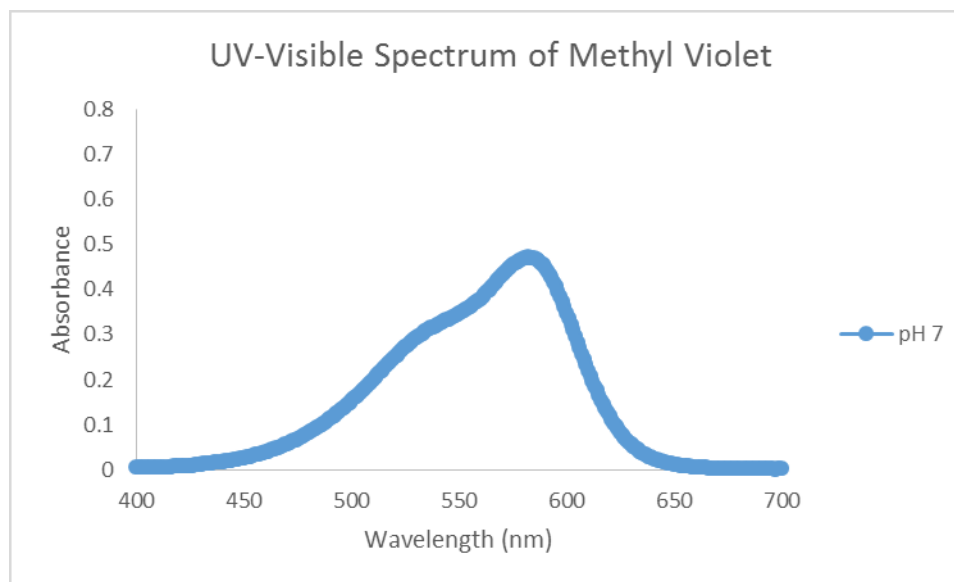


Figure 4.9 UV-visible spectrum of Methyl Violet

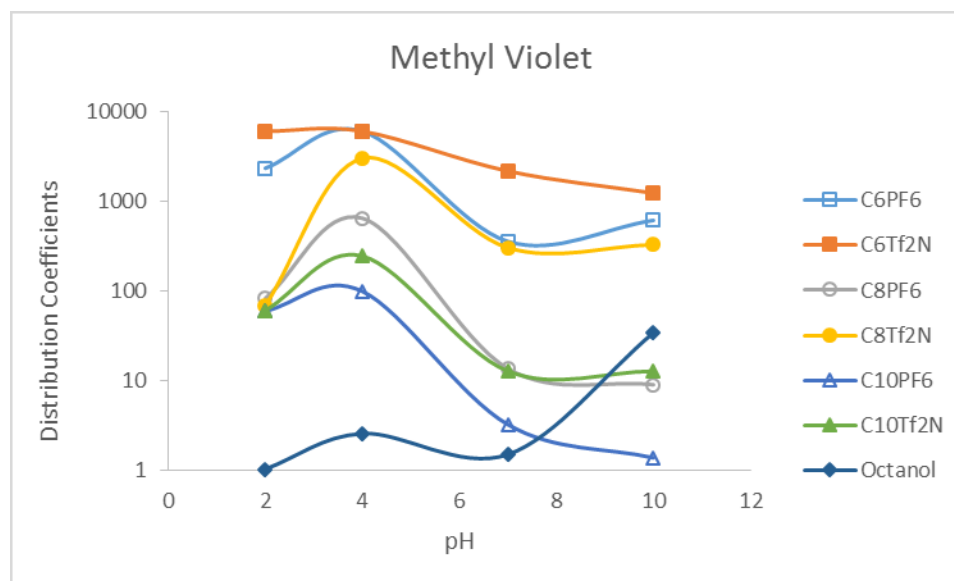


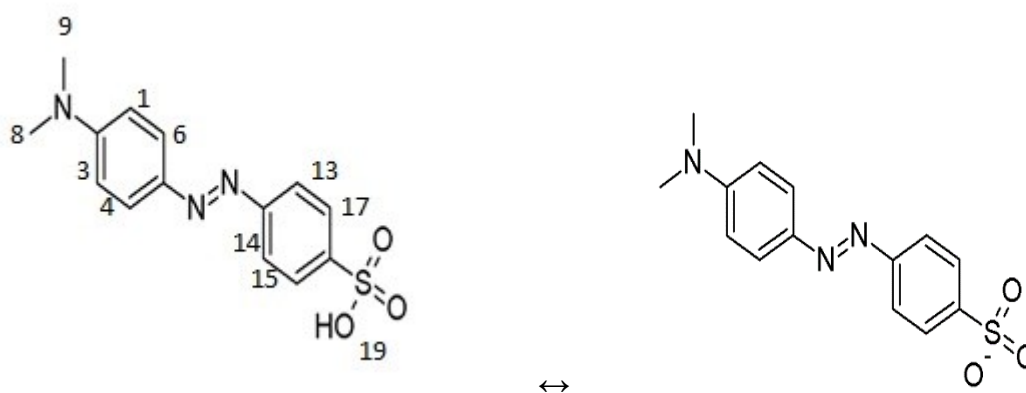
Figure 4.10 Distribution coefficient vs pH for Methyl Violet

4.3.4 Methyl Orange Extraction

Of the anionic dyes considered here, Methyl Orange (MO) is among the simpler. That is, it exists in only two forms (Figure 4.11), one protonated and the other not, their relative proportion at any given pH governed by a single pK_a (3.46) (UV-visible spectra

of neutral (pH 2) and anionic (pH 7) forms, Figure 4.12). Figure 4.13 shows a fractional composition diagram for this dye. As shown, at pH values below *ca.* 3.5, MO exists predominantly in the neutral form, while above this pH, MO⁻ predominates.

Figure 4.14 shows the dependencies of D_{dye} on pH for MO.



pKas at the following atoms [4.3]:

- C1—34.0
- C3—34.0
- C4—31.8
- C6—31.8
- C8—37.2
- C9—37.2
- C13—27.1
- C14—27.1
- C15—26.1
- C17—26.1
- O19—3.5

Figure 4.11 Methyl Orange

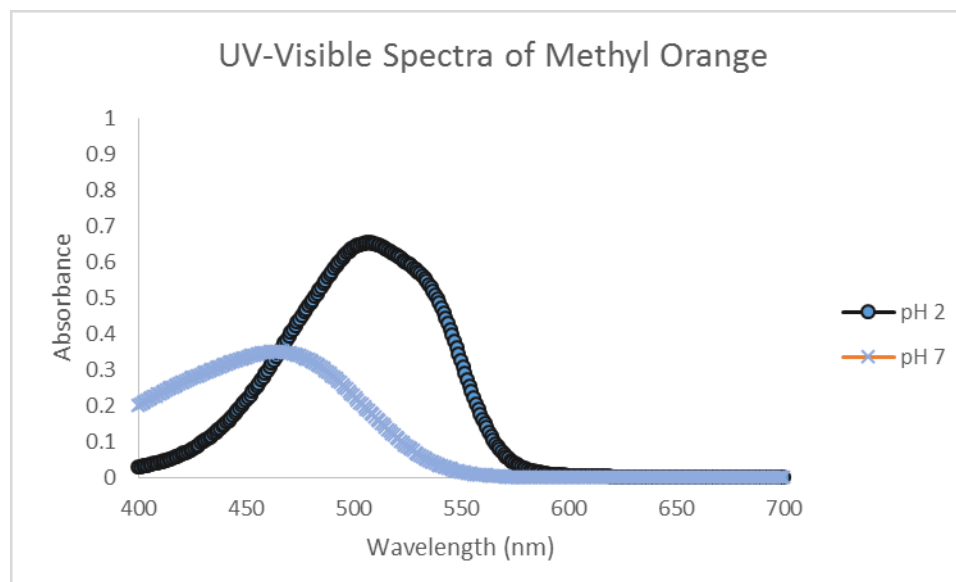


Figure 4.12 UV-visible spectra of Methyl Orange

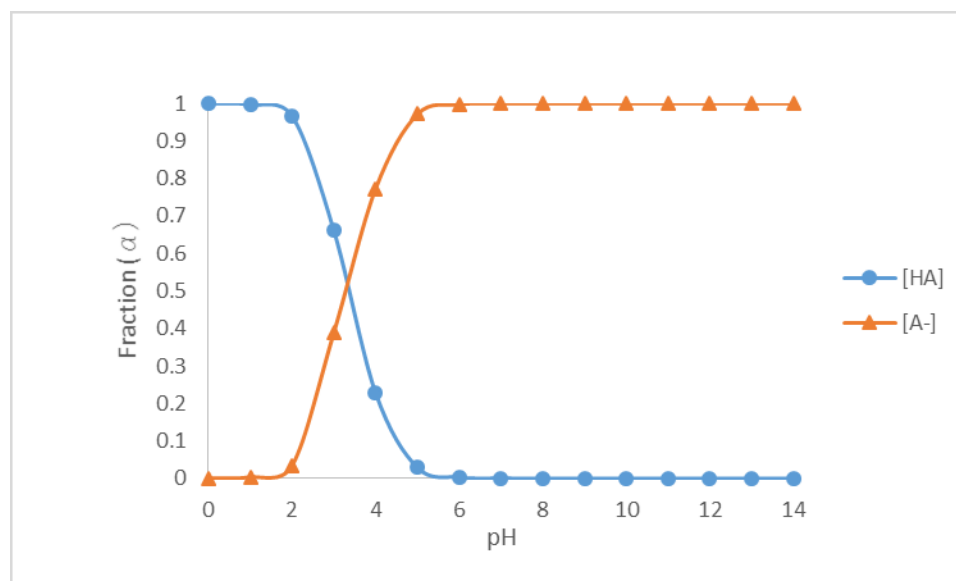


Figure 4.13 Fractional composition diagram for Methyl Orange (α vs pH)

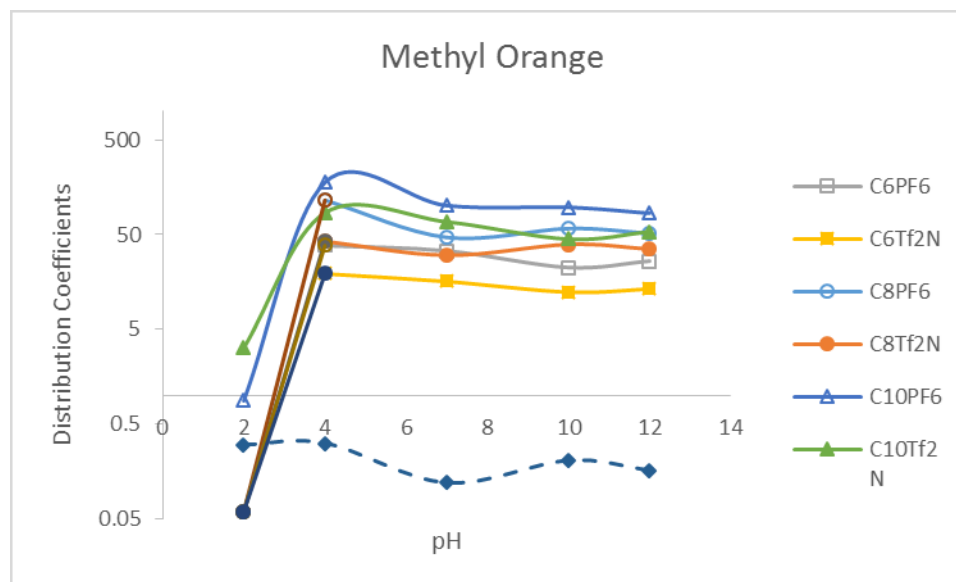


Figure 4.14 Distribution coefficient vs pH for methyl Orange

As can be seen, higher values of D_{dye} are obtained at higher pH than at low, consistent with the preferential extraction of the MO^- form. Note too that above a pH of *ca.* 4-6, the D_{dye} values are essentially constant, consistent with the fact that essentially all of the dye is in the anionic form by that pH (Figure 4.14). In contrast to MV, there was very little partitioning into octanol, regardless of pH.

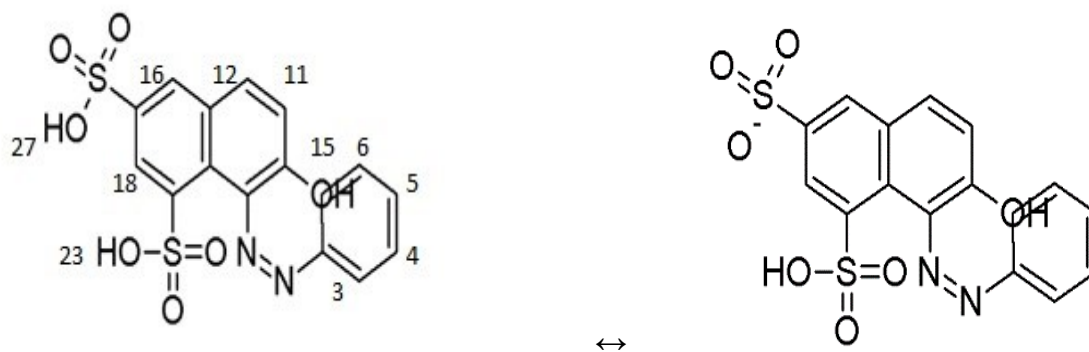
Because ILs incorporating the more hydrophilic PF_6^- anion exhibited higher extraction efficiencies than those based on the Tf_2N^- anion, anion exchange (Eqn. 4-5) undoubtedly contributes to the overall extraction process. Because D_{dye} values are not extremely large, however, it is possible that another (less efficient) process also contributes to the overall partitioning. A 2007 study by Pei *et al.* [4.5] indicates that partitioning can also be affected by hydrogen bonding interactions between the anionic dye and constituents of the IL. In the Pei study, which examined the partitioning of methyl Orange into C_6mimPF_6 and C_8mimPF_6 , it was speculated that either the

deprotonated azo group (Figure 4.11) and/or the sulfonate group experienced hydrogen-bonding with the hydrogens of the imidazolium cation [4.4].



4.3.5 Orange G Extraction

Like Methyl Orange, Orange G (OG) exists in two forms (Figure 4.15), one neutral and the other not, their relative properties at any given pH dictated by its pK_a (9.0) (UV-visible spectra of neutral and anionic forms, Figure 4.16). Figure 4.17 shows the fractional composition diagram for the dye. As indicated there, at pH values below *ca.* 9, OG exists predominantly in the neutral form, while at high pH, the anionic OG⁻ predominates. Figure 4.18 depicts the dependence of D_{dye} on pH for OG. It is immediately apparent that the distribution ratios for this dye exhibit a trend opposite that of MO. That is, OG is modestly extractable at acidic and neutral pH, but this extractability declines as the pH is raised to above the pK_a . Interestingly, the D_{dye} values are generally quite low (with the exception of those for $C_{10}\text{mimPF}_6$). In fact, data for only three ILs are included here because these were the only ILs that demonstrated any appreciable extraction ability. No measureable extraction into octanol was observed. These data are consistent with those of Pei *et al.* [4.5], who suggested that Orange G, like MO, also partitions through hydrogen bonding. In this instance, the hydroxyl group could hydrogen bond with PF_6^- . However, above the pK_a , that hydrogen will have been removed and thus the likelihood of favorable hydrogen-bonding interactions decreases sharply.



pKas at the following atoms [4.3]:

C3—31.5
 C4—33.6
 C5—33.9
 C6—33.6
 C11—27.9
 C12—28.6
 O15—11.7
 C16—23.6
 C18—21.6
 O23—9.0
 O26—9.0

Figure 4.15 Orange G

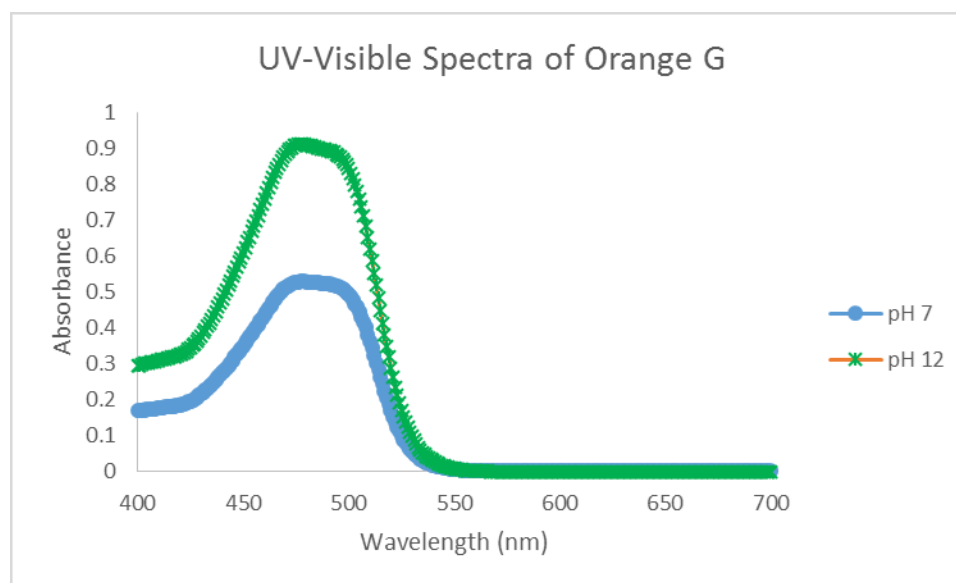


Figure 4.16 UV-visible spectra of Orange G

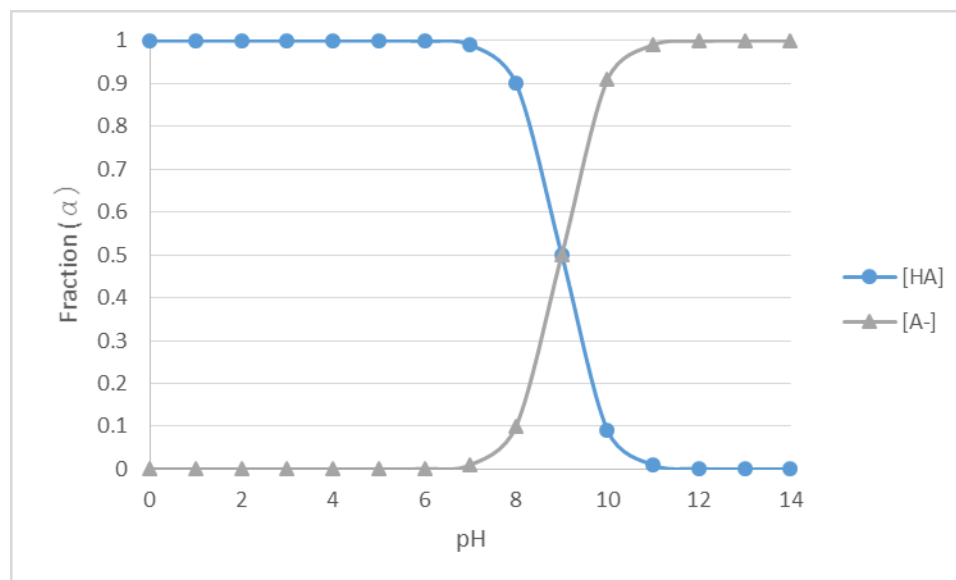


Figure 4.17 Fractional composition diagram for Orange G (α vs pH)

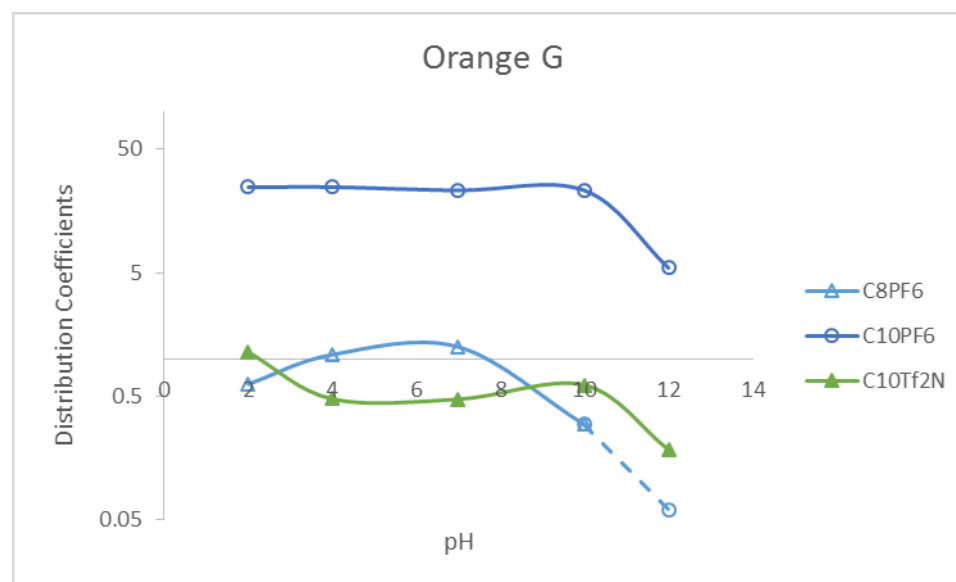
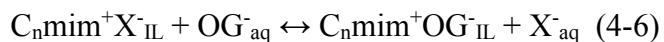


Figure 4.18 Distribution coefficient vs pH for Orange G

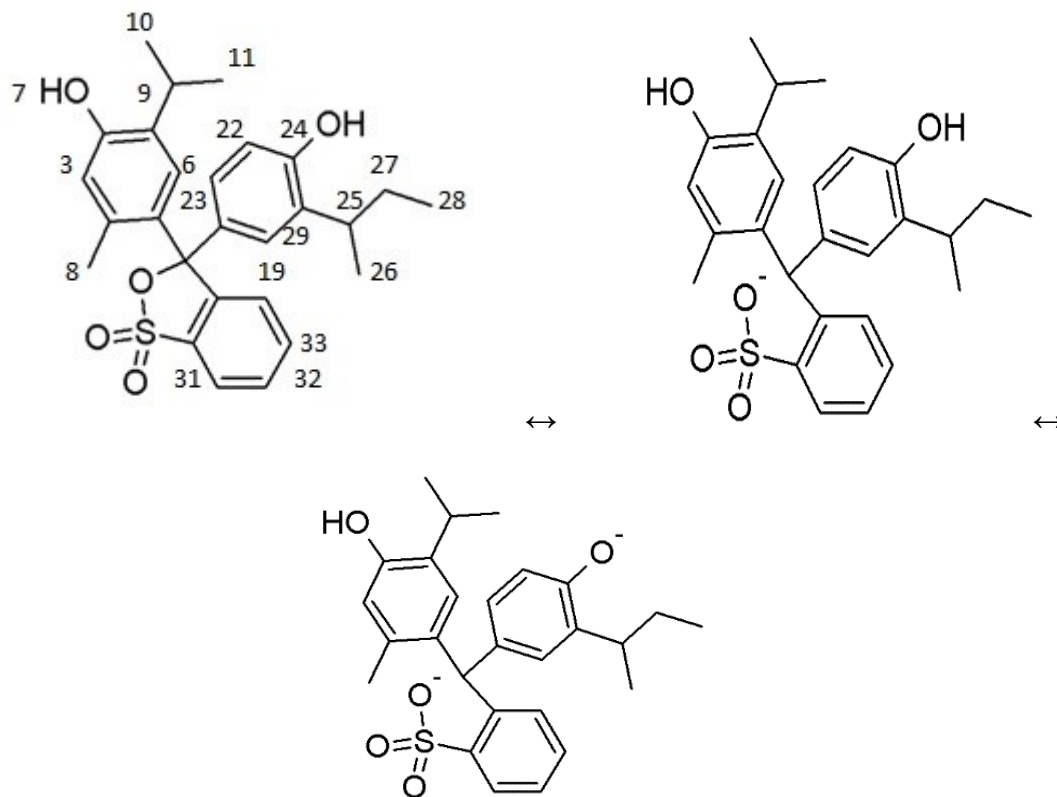
That extraction is greatest for $C_{10}\text{mimPF}_6$ than for the corresponding $C_8\text{mim}^+$ IL, and that extraction into $C_6\text{mim PF}_6$ is immeasurably low lends support to the notion that anion exchange (Eqn. 4-6) also contributes to the observed partitioning behavior. That is, as the IL cation hydrophobicity rises, the water solubility of the IL declines. Thus, less

IL anion (here, PF_6^-) is present in the aqueous phase initially, favoring a process such as that depicted in Eqn. 4-6 that leads to dissolution of PF_6^- as the dye partitions.



4.3.6 Thymol Blue Results

Thymol Blue (TB) is a relatively complex dye, as it has two pK_a s and thus three possible structures depending upon pH (Figure 4.19). A fractional composition diagram for this dye is shown in Figure 4.20, while the UV-visible spectra for the various forms of the dye are shown in Figure 4.21. As can be seen, the neutral form of Thymol Blue dominates at pH levels below the first pK_a (approximately $\text{pH} = 1.7$), the intermediate (monoanionic) form dominates between the two pK_a s (from a pH of 1.7 to 8.9), and the dianionic form dominates above the second pK_a , 8.9.



pKas of following atoms [4.3]:

C3—33.8
C6—34.1
O7—10.0
C8—37.9
C9—46.2
C10—51.2
C11—51.2
C19—33.7
C22—33.2
C23—34.0
O24—9.9
C25—45.5
C26—51.5
C27—52.9
C28—51.3
C29—30.4
C31—28.2
C32—31.2
C33—30.6

Figure 4.19 Thymol Blue

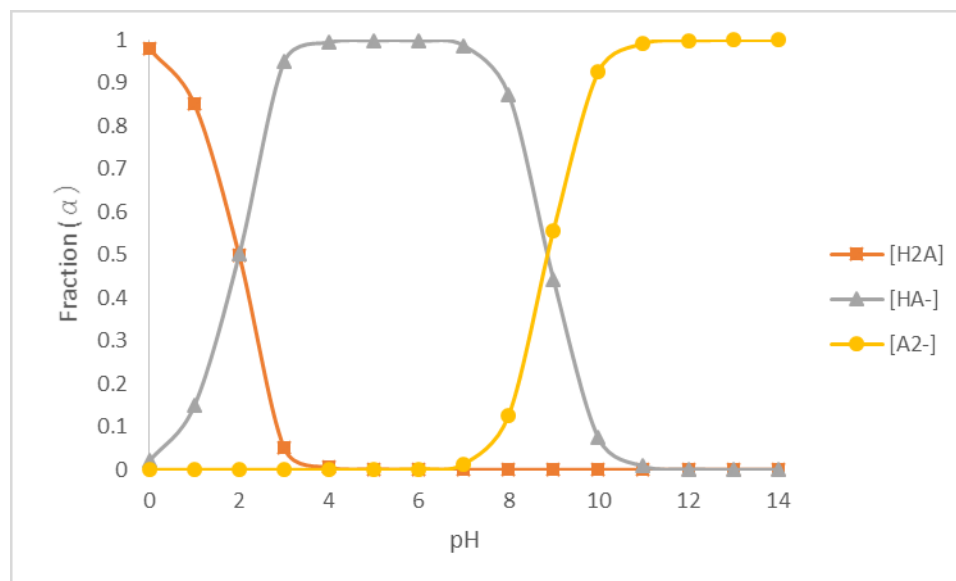


Figure 4.20 Fractional composition diagram for Thymol Blue (α vs pH)

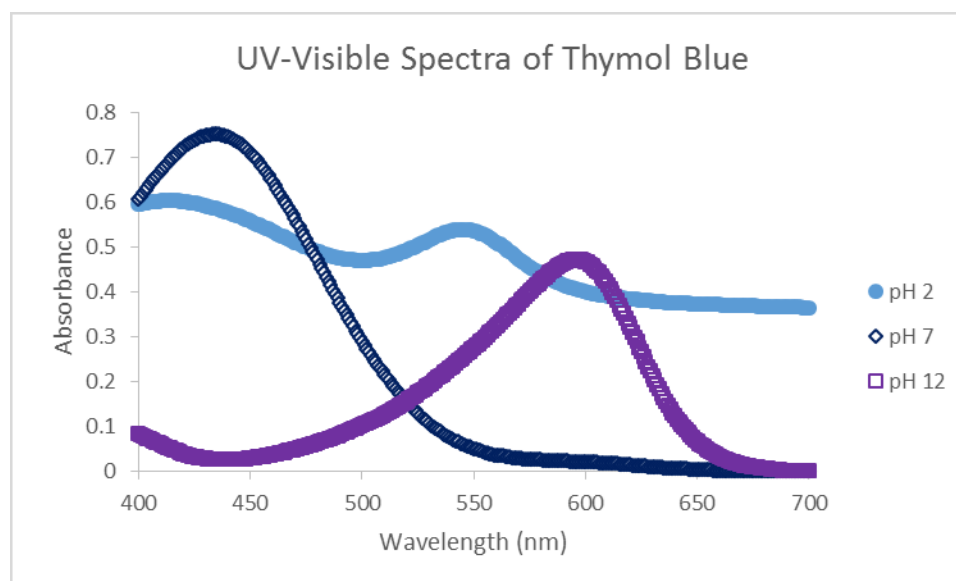
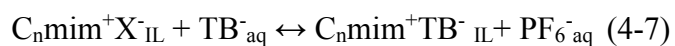


Figure 4.21 UV-visible spectra of Thymol Blue

The distribution coefficients for Thymol Blue in the various ILs followed a consistent trend. That is, partitioning was readily measurable until a pH of *ca.* 12, at which point a significant drop in D_{dye} was seen. Apparently then, the dianionic form of

the dye that dominates at this pH is not well extracted into any of the ILs examined. Given the high ionicity of ILs, it is somewhat unexpected that this form of the dye would not be extracted efficiently. In contrast, the D_{dye} values for octanol showed a consistent downward trend, decreasing as the pH increased, again indicating that in conventional solvents, it is the neutral form of the dye that is preferentially extracted. These observations are consistent with those of Visser *et al.*, who saw a sharp decline in TB partitioning at a pH of 12 and above [4.6].

The extraction data (Figure 4.22) demonstrate that the most efficient ILs for Thymol Blue across all pH levels are those that contain the largest cation, $C_{10}\text{mim}^+$. The ILs that incorporate the smaller cations exhibit lower D_{dye} values, as shown in Figure 4.22. Here again, ILs with the most hydrophobic cations exhibit the lowest aqueous solubility. Thus the initial (pre-extraction) aqueous concentration of the IL anion is smallest, thereby favoring anion exchange (Eqn 4-7). Higher D_{dye} values were also observed for ILs possessing the PF_6^- anion, particularly when paired with a large cation. Interestingly, the difference between the anions tends to lose significance when the cation size decreases, indicating that the cation size is more critical in determining extraction ability in this system.



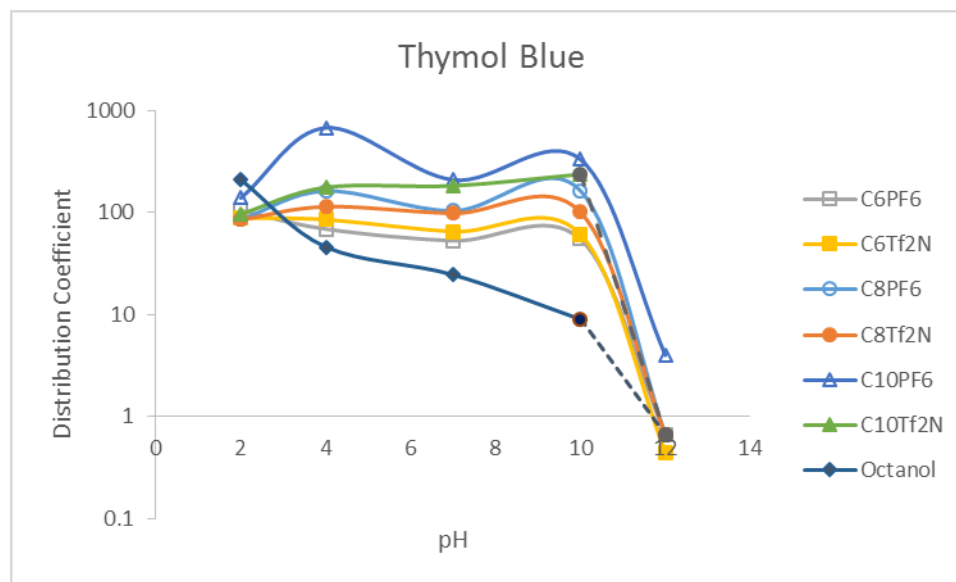


Figure 4.22 Distribution coefficient vs pH for Thymol Blue

4.4 Effect of Viscosity on Extraction Efficiency

A study conducted in 2007 by Mahmoud *et al.* [4.7] suggested that the more viscous the solvent, the higher the D_{dye} . It may be reasonable to assume, then, that the more viscous the IL the more efficiently it would extract dyes. Increasing IL cation size is normally accompanied by an increase in viscosity [4.8]. In addition, the choice of IL anion can significantly influence viscosity. The ILs comprising the C_6mim^+ cation have viscosities of 560-585 centipoise (cP) in combination with the PF_6^- anion and 87.3 with the Tf_2N^- anion [4.8]. The least viscous ILs extracted the cationic dyes the most efficiently, with D_{dye} being slightly higher for $\text{C}_6\text{mimTf}_2\text{N}$ than for C_6mimPF_6 . The ILs incorporating the C_8mim^+ cation had viscosities that were in the middle of the three cations examined (with 682-710 cP for PF_6^- and 119.3 cP for Tf_2N^-). Those ILs consisting of the $\text{C}_{10}\text{mim}^+$ cation were the most viscous, with $\text{C}_{10}\text{mimTf}_2\text{N}$ having a viscosity of 152.8 cP [4.8]. (The viscosity for $\text{C}_{10}\text{mimPF}_6$ was unavailable, however, based on the trend for the previous cations, it is reasonable to estimate that its viscosity

would be between ~780 and 880). These most viscous ILs extracted the anionic dyes the most efficiently, with $C_{10}\text{mimPF}_6$ outperforming the other ILs.

The relationship between viscosity and extraction efficiency appears to be strong but is likely coincidental. The viscosity of an IL is affected by the hydrophobicity of its constituent cation and anion, which are much more likely to predict extraction ability than a simple measure of viscosity. While this does not discredit the 2007 study, to suggest that viscosity alone will predict the extraction ability of an IL is simplistic.

4.5 Dye Stripping

For ionic liquids to be feasible for dye removal from wastewater, it is imperative that extracted dye be recoverable from the ionic liquid, permitting its recycling and reuse. To determine if extracted dyes can indeed be recovered, samples (1 mM) of Methyl Orange- and Methylene Blue-loaded IL phases ($C_8\text{mimPF}_6$ and $C_8\text{mimTf}_2\text{N}$) were subjected to a variety of stripping agents (1 M HCl, 0.1 M NaOH, and a 50% (v/v) ethanol:water mixture) in an attempt to remove the dye. Previous work with these stripping agents has demonstrated that they are effective at removing certain dyes (Methyl Orange, Eosin Yellow, and Orange G) from imidazolium-based ILs. Specifically, Pei *et al* [4.5] were successful in removing 97.5% and 96.2% of Methyl Orange from $C_6\text{mimPF}_6$ and $C_8\text{mimPF}_6$, respectively, using 1M hydrochloric acid at a volume ratio of 0.10 (O/A). (In this experiment, samples of the same ILs saturated with Methyl Orange were treated with 1M HCl but at a 1:1 volume ratio.) Along these same lines, Vijayaraghavan *et al.* were successful in stripping dyes from ILs using a 1:1 mixture of isopropyl alcohol and water using an O/A ratio of 1:1 [4.9]. In this particular experiment, a 1:1 mixture of ethanol and water was used in an attempt to strip Methylene Blue from

the ILs of interest. A sodium hydroxide solution (0.5 M) solution was also used in an attempt to strip dyes (Methyl Orange or Methylene Blue) that had been extracted into ILs at more basic pH levels.

Curiously, our attempts at dye stripping have thus far been unsuccessful. Methyl Orange—loaded IL was treated with the HCl, NaOH, and ethanol/water stripping agents and showed some dye removal with all of these agents; however, the IL phase remained color saturated. It appeared that the dye particles crashed out of solution after contact with a stripping agent, as solid flecks could be seen near the surface of the IL. Therefore, any subsequent addition of an aqueous stripping agent would simply re-dissolve the solid particles and contribute to color saturation. This phenomenon was seen regardless of how long the system had remained sitting before stripping, be it months or mere minutes. This may be related to the observation that a solid dye precipitate can form within the IL phase, as seen by Ali *et al.* [4.10], who were able to successfully remove solid precipitated dyes. Therefore, this phenomenon may explain the solid dye particles that were seen upon contact with an aqueous solution.

After a single stripping of Methyl Orange with the 1.0 M HCl (at an O/A ratio of 1:1), the aqueous phase was analyzed using UV-visible spectrophotometry. Two samples, one of which contained dye-saturated C₆mimPF₆ and the other dye-saturated C₈mimPF₆, were chosen in an attempt to replicate the results of Pei *et al.* [4.5]. After dilution to the point where measurement was possible (attainment of an absorbance value between 0.000 and 1.000), the concentration was calculated to be *higher* than 1 mM (i.e., 1.44 and 1.32 mM), which should be physically impossible. It is likely, then, that the higher concentration was caused by dye particles that had “crashed out” of solution.

Methylene Blue-saturated IL phases were treated with the aforementioned HCl, the 0.1 M NaOH, and the ethanol-water mix, but none were successful at stripping the dye. The volumes of the various stripping agents were increased in an attempt to force dye stripping, but in the end, only the dissolution of the IL increased, particularly with the ethanol-water mixture. These results were rather discouraging because if the dye cannot be stripped, the IL cannot be reused.

4.6 Conclusions

The objective of this work was to determine the characteristics of ionic liquids and of dyestuffs that favor efficient extraction of a dye from aqueous solution and its facile recovery. The results obtained show that structural differences between anionic and cationic dyes lead to differences in the way they are extracted by the ionic liquids. That is, extraction of anionic dyes is favored by a larger IL cation and a less hydrophobic anion, while the extraction of cationic dyes is favored by smaller IL cations and more hydrophobic anions. Of the ILs considered, those incorporating C_8mim^+ appear to come closest to an “all purpose” solvent, extracting all dyes except Orange G, regardless of IL anion. The difficulties encountered in recovering the extracted dyes, however, was discouraging. Although previous researchers have reported success in stripping dyes from some of the ionic liquids, our experience has not been as positive. Thus a simple and inexpensive method to efficiently strip extracted dyes remains to be identified.

4.7 References

- 4.1 Deetlefs, M., & Seddon, K.R. "Improved preparations of ionic liquids using microwave irradiation". *Green Chemistry*, **2003**, *5*, 181-186.
- 4.2 Huddleston, J.G., Willauer, H.D., Swatloski, R.P., Visser, A.E., and Rogers, R.D. "Room temperature ionic liquids as novel media for 'clean' liquid-liquid extraction". *Chem. Communications*, **1998**, 1765-1766.
- 4.3 ACE and JChem acidity and basicity calculator. Epoch.uky.edu/ace/public/pKa.jsp. Accessed 6 May 2014.
- 4.4 Garvey, S.L., and Dietz, M.L. "Ionic liquid anion effects in the extraction of metal ions by macrocyclic polyethers". *Separation and Purification Technology*, **2014**, *123*, 145-152.
- 4.5 Pei, Y.C., Wang, J.J., Xuan, X.P., Fan, J., and Fan, M. "Factors Affecting Ionic Liquids Based Removal of Anionic Dyes from Water". *Environmental Science & Technology*, **2007**, *41* (14), 5090-5095.
- 4.6 Visser, A.E., Swatloski, R.P., and Rogers, R.D. "pH-Dependent partitioning in room temperature ionic liquids". *Green Chemistry*, **2000**, 1-4.
- 4.7 Mahmoud, A.S., Ghaly, A.E., and Brooks, M.S. "Removal of dye from textile wastewater using plant oils under different pH and temperature conditions". *American Journal of Environmental Sciences*, **2007**, *3* (4), 205-218.
- 4.8 Zhang, S., Sun, N., He, X., Lu, X., and Zhang, X. "Physical properties of ionic liquids: database and evaluation". *Journal of Physical Chemistry*, **2006**, *35* (4), 1475-1517.
- 4.9 Vijayaraghavan, R., Vedaraman, N., Surianarayanan, M., and MacFarlane, D.R. "Extraction and recovery of azo dyes in an ionic liquid". *Talanta*, **2006**, *69*, 1059-1062.
- 4.10 Ali, M., Sarkar, A., Pandey, M.D., and Pandey, S. "Efficient precipitation of dyes from dilute aqueous solutions of ionic liquids". *Analytical Sciences*, **2006**, *22*, 1051-1053.

CHAPTER 5: ASSESSMENT OF ENVIRONMENTAL FRIENDLINESS— CONCLUSIONS AND RECOMMENDATIONS

5.1 Assessment of Environmental Friendliness

The wastewater generated by textile mills is contaminated by several components, not only by dyes. While several methods exist for the cleanup of these wastewaters, most of them have drawbacks such as high cost, inefficiency, and time consumption [5.1].

Ionic liquids may offer at least a partial solution, offering efficient and rapid extraction of dyes from wastewaters.

Originally most ionic liquids were thought to be “green” due to their negligible vapor pressures. Subsequent work, however, demonstrated that their ionic components (*e.g.*, PF_6^-) can be just as threatening to aquatic environments as the dyes they are trying to remove. Preliminary research indicates that ionic liquids with smaller cations and non-halogenated anions may be non-toxic and therefore safe to introduce into an aquatic environment [5.2-5.4]. Since the number of possible combinations of anions and cations is extremely large and the library of ILs is ever growing, it is likely that many truly environmentally benign ILs will be identified.

Because they incorporate fluorinated anions, the ionic liquids studied in Chapter 4 are not environmentally friendly, but they are easy to synthesize and their properties are well understood. All of the ILs exhibited the ability to extract a variety of dyes, both cationic and anionic, with varying amounts of efficiency. Mechanisms for the extraction were also proposed, with the highest distribution coefficients likely the result of a cation- or anion-exchange mechanism. Thus, the anionic or cationic component of the IL may be transferred into the aqueous phase as the dye is extracted.

In an effort to confirm that the IL is indeed lost to the aqueous phase during dye extraction (and thus, to validate the ion-exchange mechanism proposed), the NMR spectra of the aqueous phases remaining after extraction of Methylene Blue, Safranin O, and methyl Violet were compared to the spectra for the ILs employed and to the aqueous phases prior to extraction. A typical result is presented in parts a-c of Figure 5.1 (see Appendix for remaining spectra). In general, the spectra of the dyes tended to exhibit one major peak between 3 and 4 ppm, while the spectra of the ILs had several peaks in the region of 0-5 and 7-10 ppm. All of the post-extraction aqueous phases examined showed major peaks only between 3 and 4 ppm; however, these peaks were not clear singlets like those in the pre-extraction dye spectra. Because the ILs also have peaks in the same range, it is possible that the spectral evidence indicating the presence of an IL is masked. No peaks at ca. 9 ppm were observed, however, consistent with the absence of the imidazolium cation in the aqueous phase.

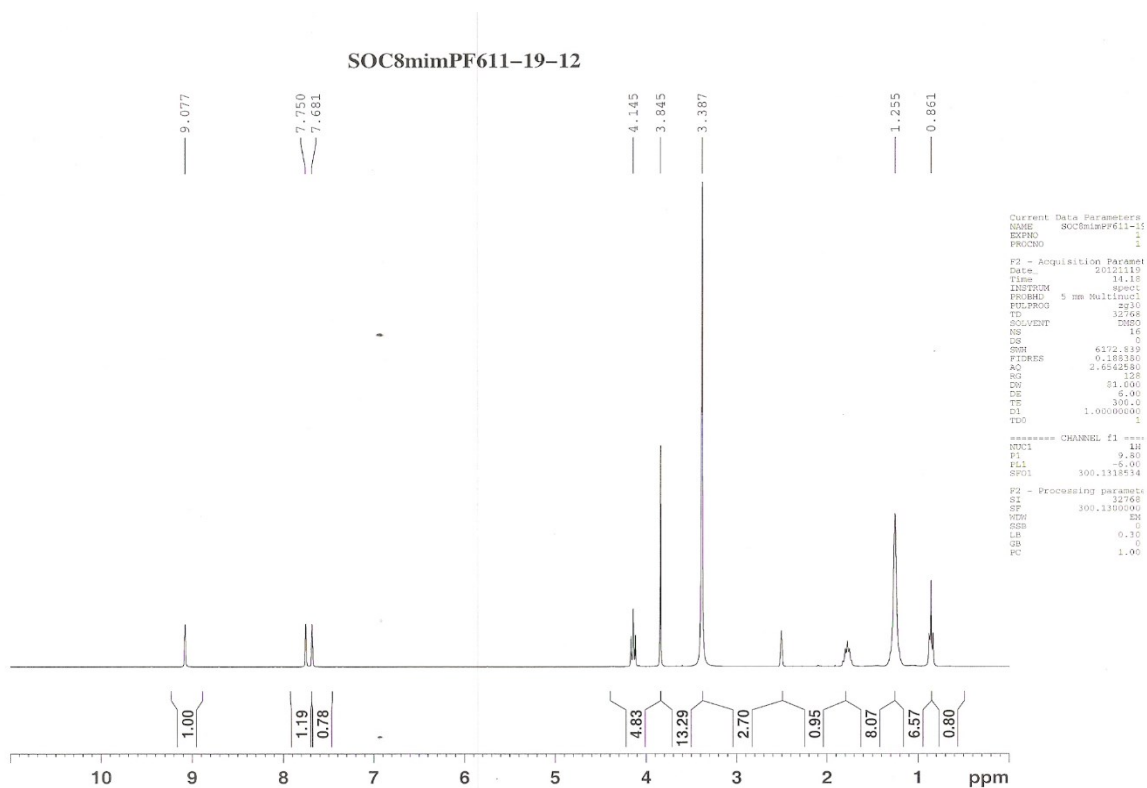


Figure 5.1A NMR spectrum of C₈mimPF₆ in DMSO

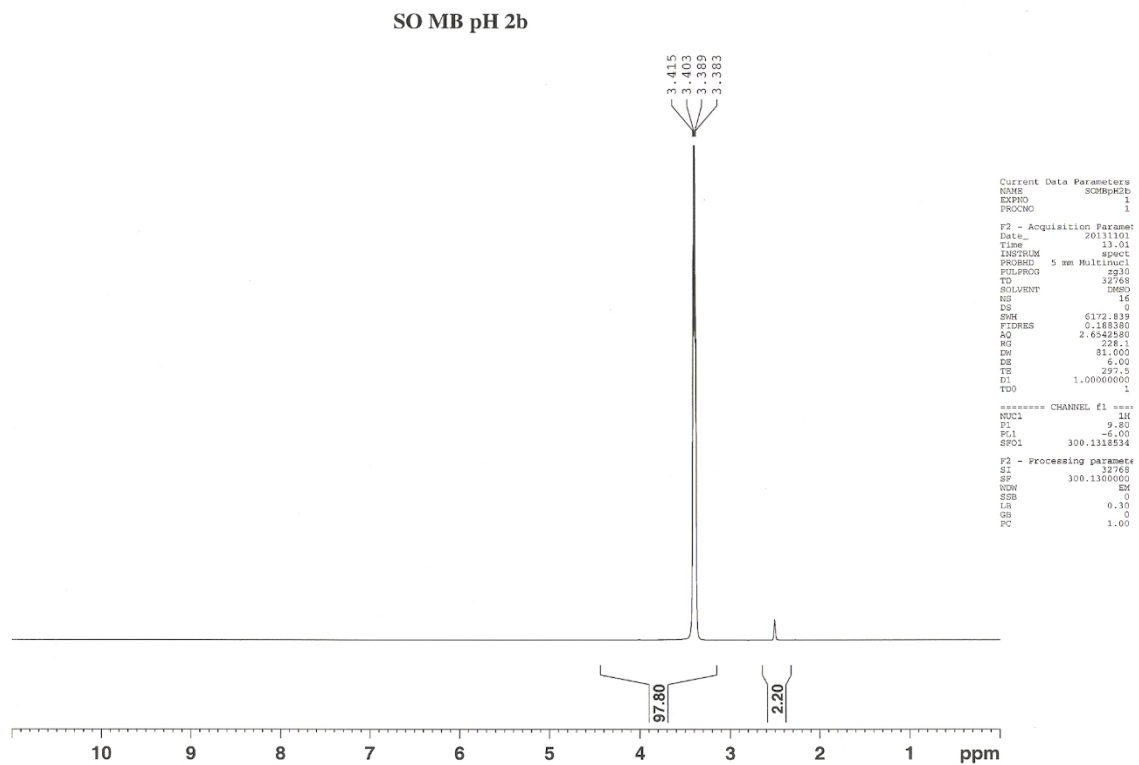


Figure 5.1B NMR spectrum of Methylene Blue in DMSO

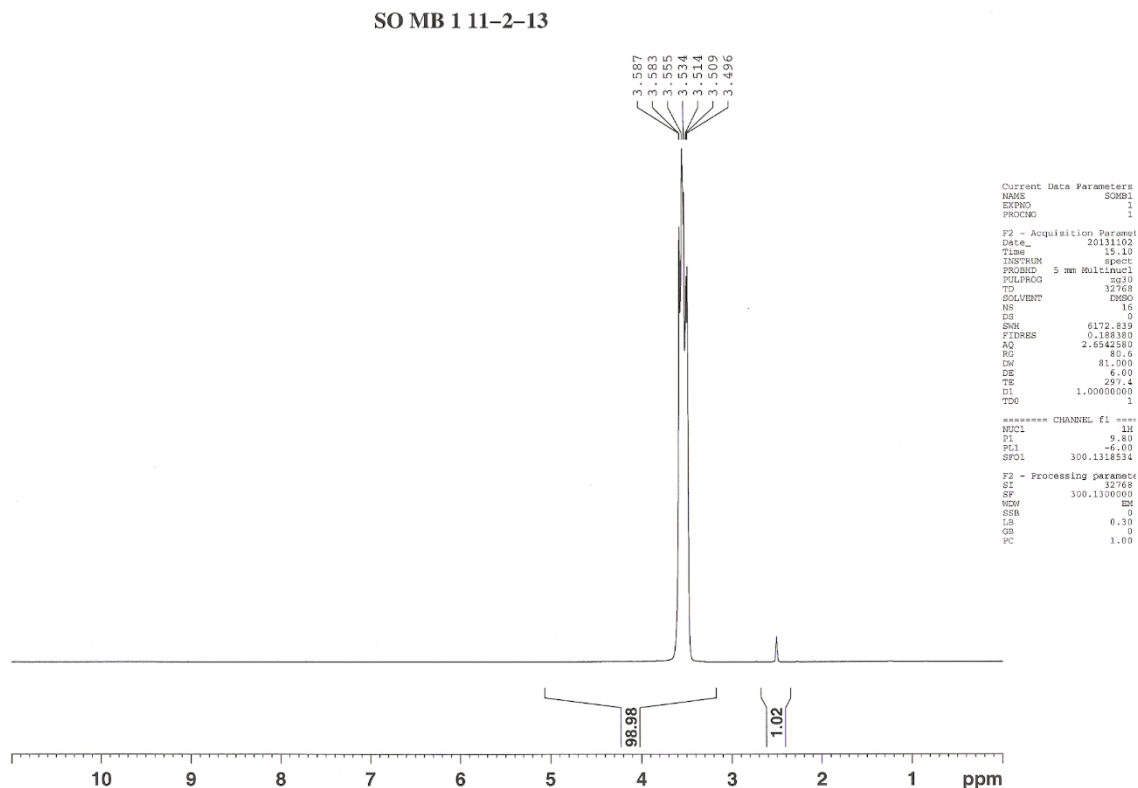


Figure 5.1C NMR spectrum of aqueous phase of MB1, pH 2, C₈mimPF₆

Evidence of IL loss upon anionic dye extraction was more readily obtained.

First, F-19 NMR spectra were obtained for samples of KPF₆ and LiTf₂N and the peaks associated with these compounds determined [5.5-5.6]. The Bruker DPX 300 NMR was again used, here with the F-19 probe. Fluorine-19 spectra were then obtained for two aqueous, post-extraction samples—one was of Thymol Blue, pH 4, originally contacted with C₆mimPF₆ and the other was Methyl Orange, pH 7, originally contacted with C₆mimTf₂N. All samples were diluted in deuterium oxide (Sigma Aldrich, Milwaukee, WI). These spectra were compared with spectra of the appropriate IL. As seen, the PF₆⁻ anion has two peaks between -70 and -75 ppm, which are evident in the Thymol Blue spectrum (along with an unexplained peak at -90 ppm). The Tf₂N⁻ anion has two peaks centered around -100 ppm, which are evident in the methyl Orange sample as well. The

presence of the anion peaks in both the Thymol Blue and methyl Orange spectra suggests that the IL was indeed lost to the aqueous phase during dye extraction.

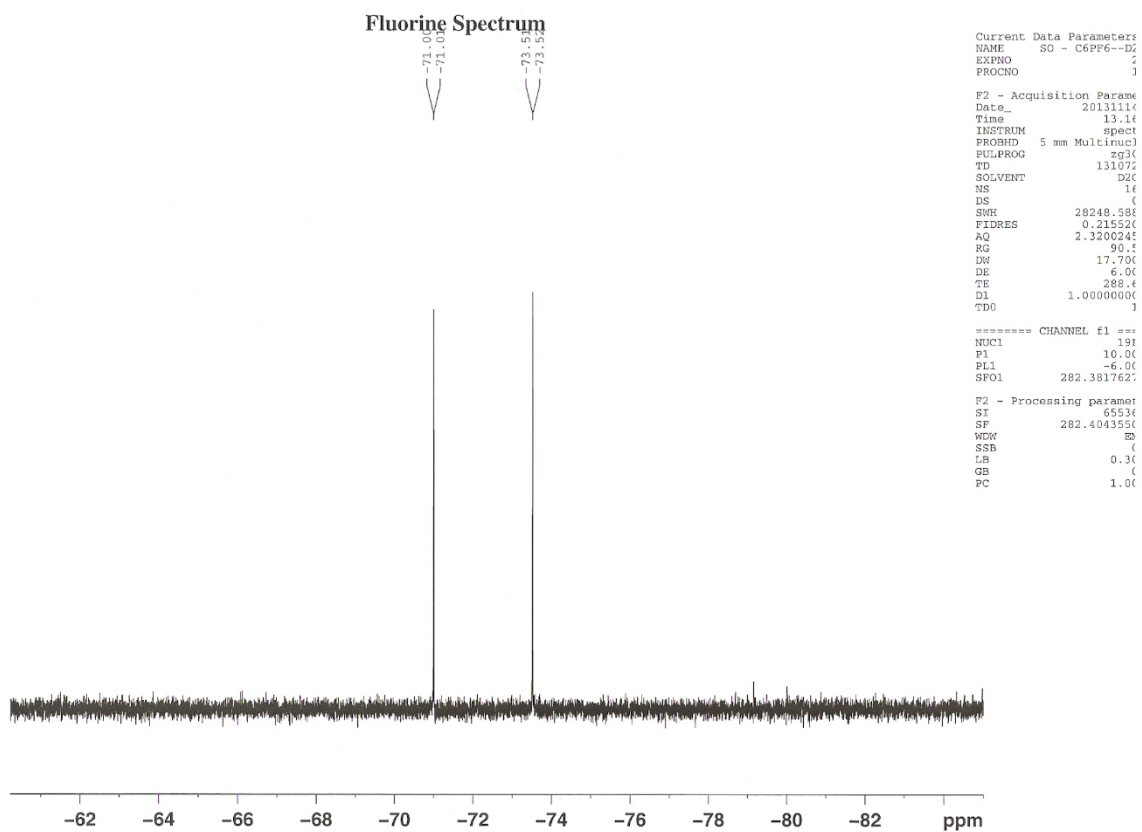


Figure 5.2 Fluorine-19 spectrum of C₆mimPF₆

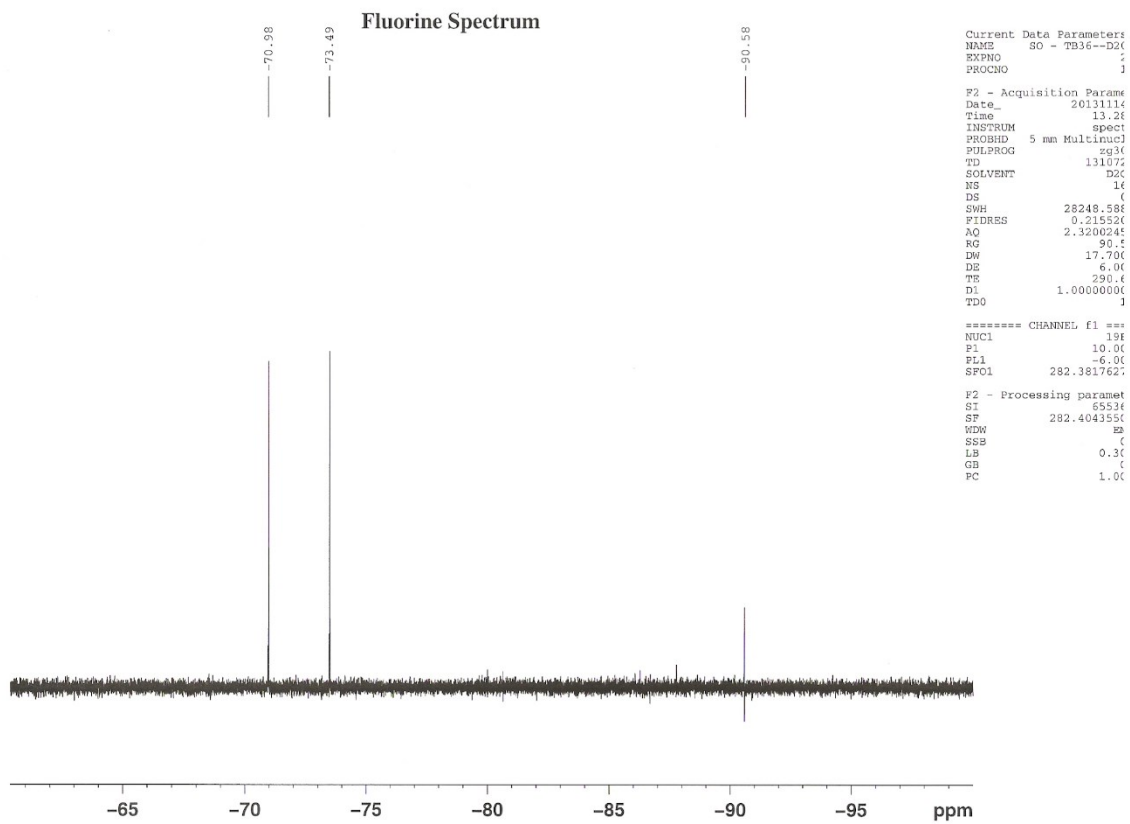


Figure 5.3 Fluorine-19 spectrum of TB36, pH 7, C₆mimPF₆

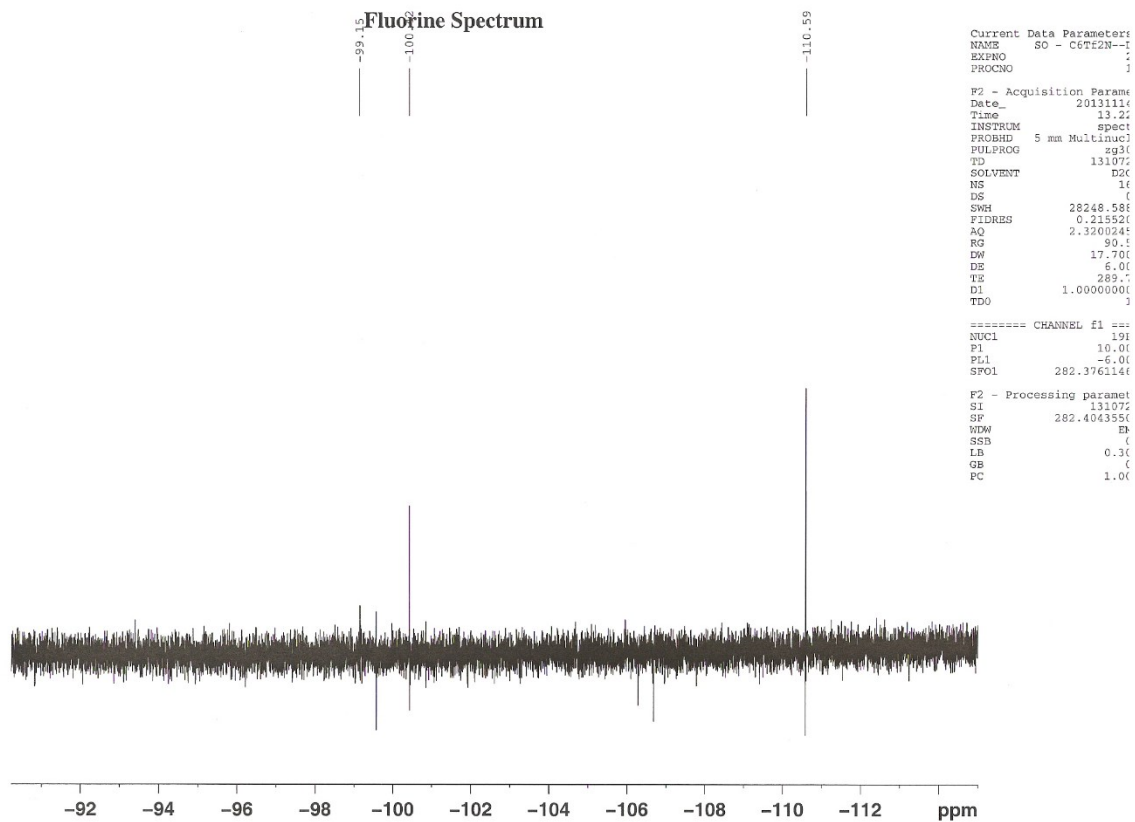


Figure 5.4 Fluorine-19 spectrum of C₆mimTf₂N

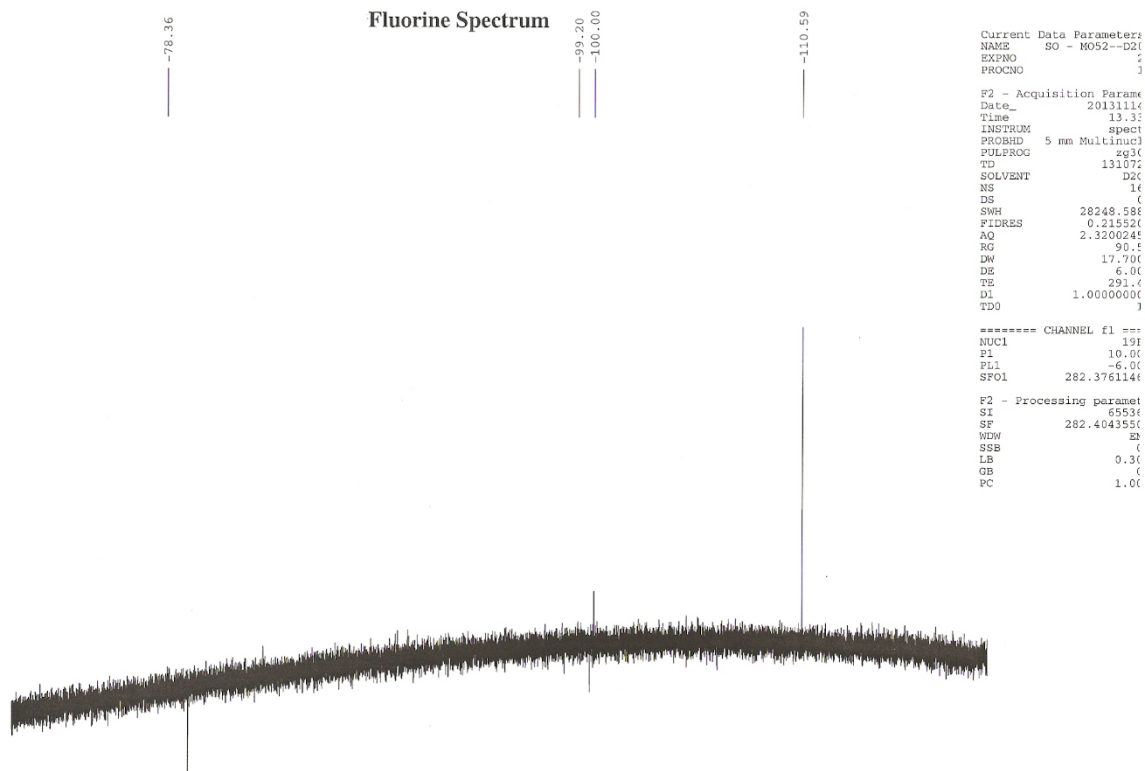


Figure 5.5 Fluorine-19 spectrum of MO52, pH 7, C₆mimTf₂N

Because fluorinated anions markedly increase the toxicity of an IL, it is highly desirable (where feasible) to employ ILs incorporating non-fluorinated anions. Similarly, imidazolium cations are not regarded as environmentally benign. Here too then, the use of other, less toxic cations would be preferred in a large-scale waste treatment application. With this in mind, we have carried out a preliminary examination of tri(hexyl)tetradecylphosphonium chloride ($P_{6,6,6,14}^+ Cl^-$), an IL previously proposed as the basis for the process-scale separation of cobalt from nickel [5.7]. Specifically, the extraction of three anionic dyes (*i.e.*, Thymol Blue, Methyl Orange, and Orange G) and a cationic dye (Methylene Blue) was studied, following the procedures outlined above (Ch. 4, Sec 2). Not unexpectedly, $P_{6,6,6,14}^+ Cl^-$ failed to extract any measurable quantity of Methylene Blue, a likely result of the fact that extraction would require exchange of the

dye cation for the highly hydrophobic phosphonium cation. In contrast, $P_{6,6,6,14}^+Cl^-$ yielded higher D_{dye} values for Methyl Orange and Orange G than did the imidazolium ILs. Interestingly, the results for Thymol Blue (i.e., poor extraction at intermediate pH values) were the opposite of the behavior observed with the imidazolium ILs. The phosphonium extraction efficiencies are likely so different from those of the imidazoliums because of the difference in anion. The Cl^- anion is considerably more hydrophilic than that of either PF_6^- or Tf_2N^- , thus facilitating anion exchange with an anionic dye.

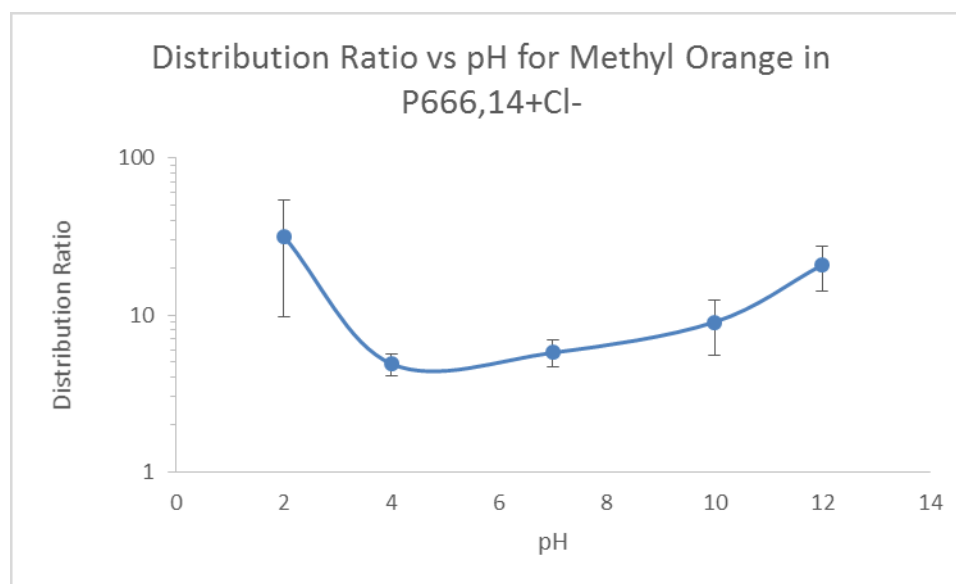


Figure 5.6 Distribution ratio for Methyl Orange in $P_{6,6,6,14}^+Cl^-$

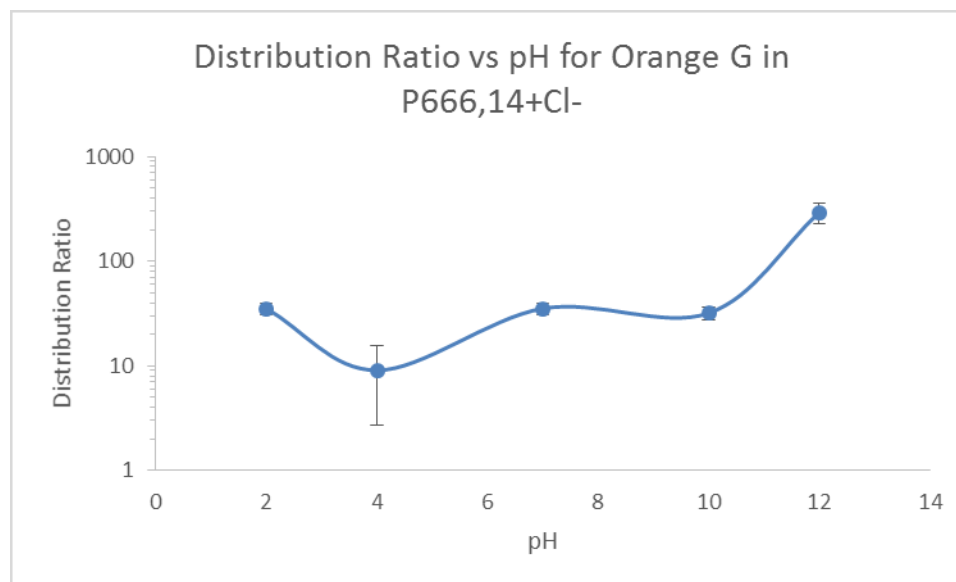


Figure 5.7 Distribution ratio vs pH for Orange G in $P_{6,6,6,14}^+Cl^-$

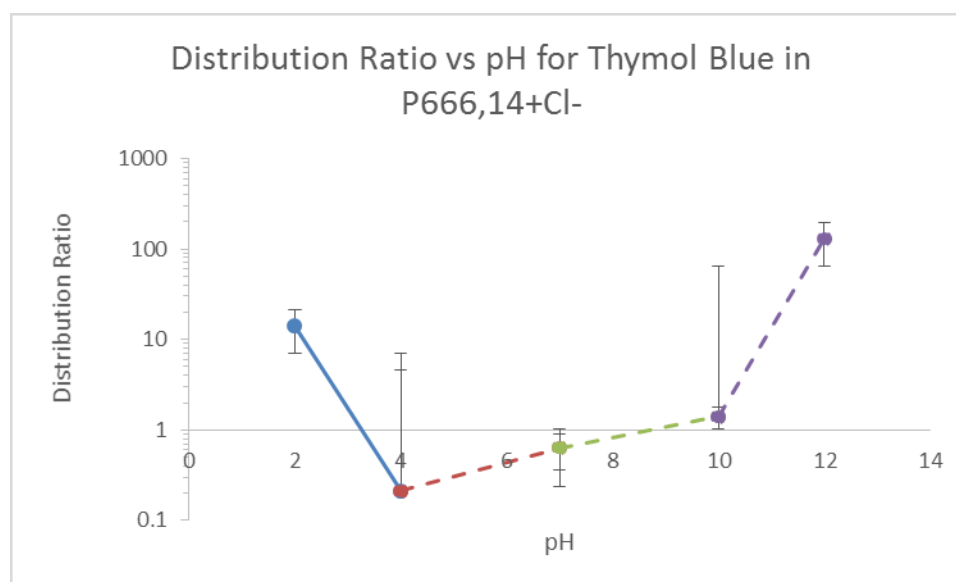


Figure 5.8 Distribution ratio vs pH for Thymol Blue in $P_{6,6,6,14}^+Cl^-$

The main drawback of $P_{6,6,6,14}^+Cl^-$ is its tendency to form an emulsion layer when contacted with an acidic aqueous phase. This can be dealt with only through lengthy centrifugation, or (if confined to a layer at the IL-aqueous interface) by its extraction. This emulsion layer was also evident when the phosphonium cation was paired with other anions such as salicylate, benzoate, and saccharinate. Thus, although this IL may be both

more “environmentally friendly” and superior to the imidazolium ILs for the extraction of certain dyes, it is clearly not optimum. In fact, dye-stripping again proved to be problematic, with no success using a sodium chloride solution at the concentrations of 0.1 M, 1 M, and even 10 M.

5.2 Recommendations

Many other ionic liquids are available for evaluation in dye extraction. Of course those that are inherently non-toxic (such as $P_{6,6,6,14}^+Cl^-$) are preferable, particularly if their synthesis can be effected by a route involving non-toxic (or less toxic) starting materials. For example, recent work has shown that hydroxyl-functionalized analogs of the imidazolium cation can be synthesized from fructose, a naturally occurring carbohydrate [5.8]. For dyes whose extraction proceeds through cation exchange, a sugar-derived imidazolium cation may represent an improvement in terms of overall process “greenness” versus a conventional imidazolium IL. Unfortunately, the synthesis of the sugar-derived IL is considerably more complicated, as illustrated in Figure 5.9. A thorough cost vs benefit analysis should be undertaken before any experimentation is conducted using this particular synthesis.

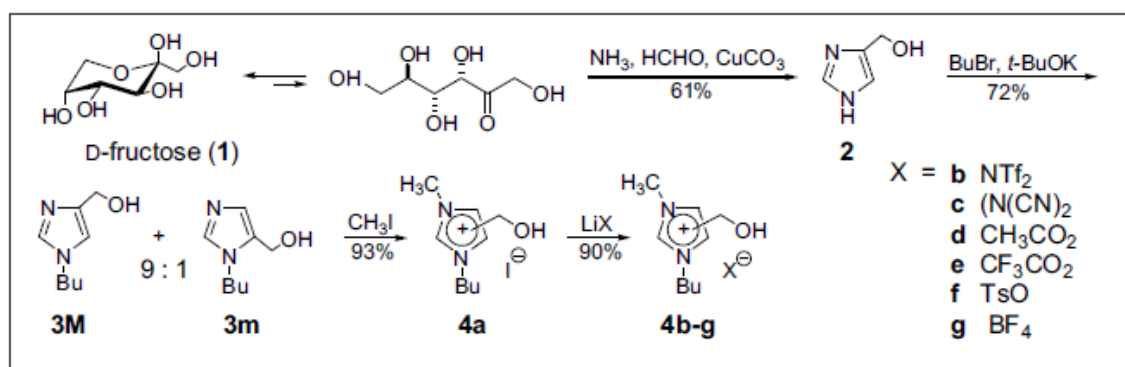


Figure 5.9 Synthesis of 1,3-disubstituted imidazolium [5.8]

It would also be useful to examine the extraction efficiencies of a variety of ILs in a combination of dyes. Textile wastewater usually contains a mixture of dyes, so it is desirable that an IL be able to extract all of them at once. Different dyes that represent a broad spectrum of properties (*i.e.*, cationic, anionic, azo-structured, reactive, *etc.*) should be utilized in extraction experiments. Most beneficial would be tests on real wastewater samples with a variety of ionic liquids. Naturally, these experiments would create issues with measurement as it would be difficult to create calibration standards due to the variety of colors and color combinations that would be encountered. Instrumentation other than UV-visible spectrometers could potentially be used once a measurement methodology can be established.

5.3 References

- 5.1 Pang, Y.L., and Abdullah, A.Z. "Current Status of Textile Industry Wastewater Management and Research Progress in Malaysia: A Review". *Clean Soil, Air, Water*, **2013**, 00 (0), 1-14.
- 5.2 Cvjetko, M., Radosevic, K., Tomica, A., Slivac, I., Vorkapic-Furac, J., and Gaurina Sreck, V. "Cytotoxic effects of imidazolium ionic liquids on fish and human cell lines". *Arh Hig Rada Toksikol*, **2012**, 63, 15-20.
- 5.3 Viboud, S., Papaiconomou, N., Cortesi, A., Chatel, G., Draye, M., and Fontvieille, D. "Correlating the structure and composition of ionic liquids with their toxicity on *Vibrio fischeri*: a systematic study". *Journal of Hazardous Materials*, **2012**, 215-216, 40-48.
- 5.4 Peric, B., Marti, E., Sierra, J., Cruanas, R., Iglesias, M., and Garau, M.A. "Terrestrial ecotoxicity of short aliphatic protic ionic liquids". *Environmental Toxicology and Chemistry*, **2011**, 30 (12), 2802-2809.
- 5.5 Freire, M. G., Neves, C. M. S. S., Marrucho, I. M., Coutinho, J. A. P., Fernandes, A.M. "Hydrolysis of tetrafluoroborate and hexafluorophosphate counter ions in imidazolium-based ionic liquids". *Journal of Physical Chemistry A*, **2010**, **114**, 3744-3749.
- 5.6 Laali, K. K., Okazaki, T., and Bunge, S. D. "*N*-(Trifluoromethylsulfonyl)aryloxytrifluoromethylsulfoximines [ArO-SO(CF₃)=NTf] and *N*-Aryltriflimides Ar-N(Tf)₂ by thermal and photolytic deiazonation of [ArN₂][BF₄] in

[BMIM][Tf₂N] ionic liquid; exploiting the ambident nucleophilic character of a ‘non-nucleophilic’ anion”. *Journal of Organic Chemistry*, **2007**, *72* (18), 6758-6762.

5.7 Wellens, S., Thijs, B., and Binnemans, K. “An environmentally friendlier approach to hydrometallurgy: highly selective separation of cobalt from nickel by solvent extraction with undiluted phosphonium ionic liquids”. *Green Chemistry*, **2012**, *14*, 1657-1665.

5.8 Marra, A., Chiappe, C., and Mele, A. “Sugar-Derived Ionic Liquids”. *Glycochemistry Today*, **2011**, *65*, 76-80.

APPENDIX A

Structures of Dyes

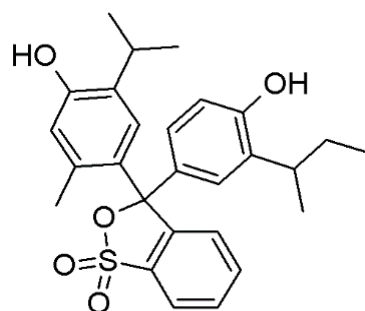


Figure A.1 Thymol Blue

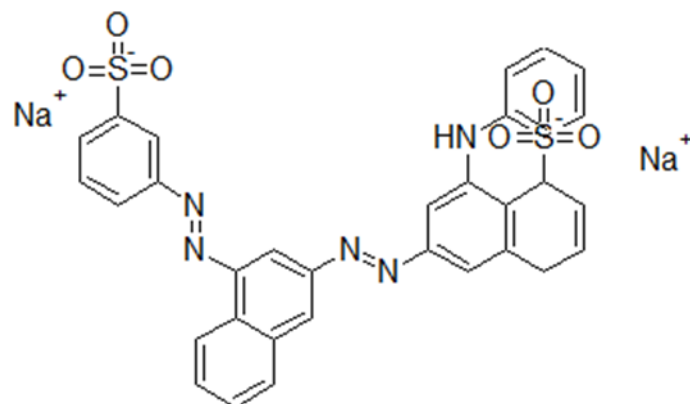


Figure A.2 Acid Blue Dye

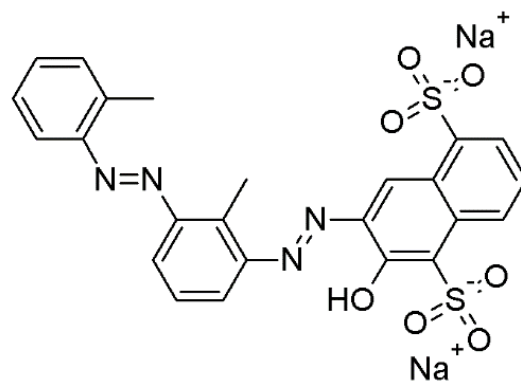


Figure A.3 Acid Red Dye

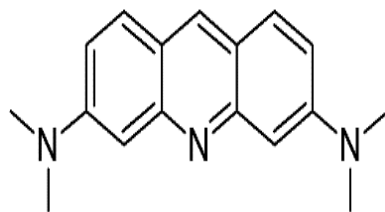


Figure A.4 Acridine Orange

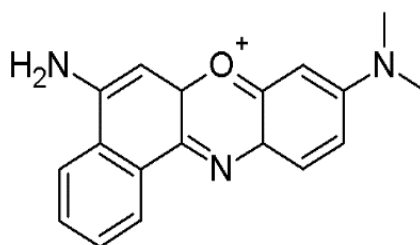


Figure A.5 Nile Blue A

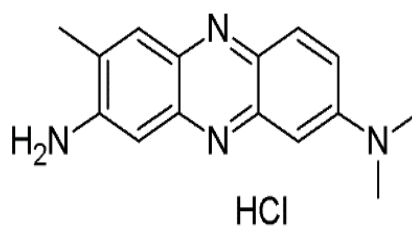


Figure A.6 Neutral Red



Figure A.7 Methylene Blue

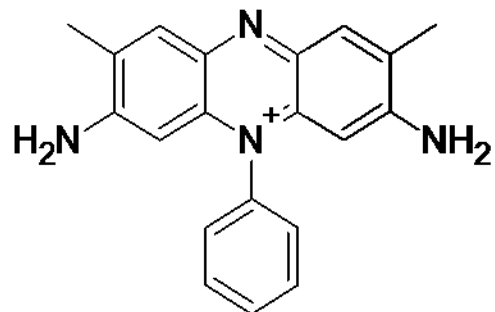


Figure A.8 Safranin O

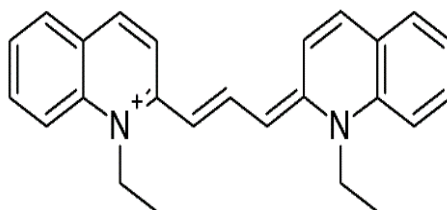


Figure A.9 Pinacyanol Chloride

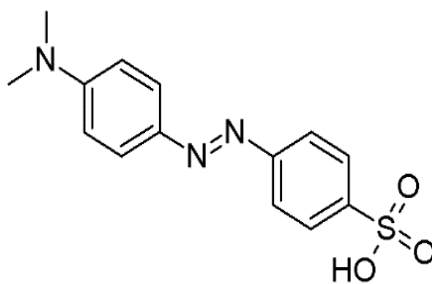


Figure A.10 Methyl Orange

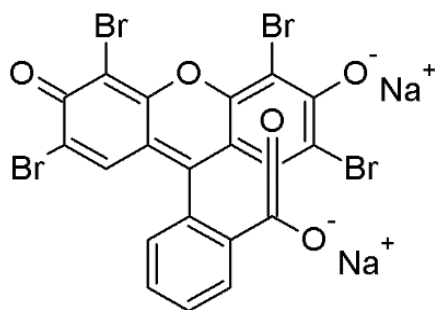


Figure A.11 Eosin Yellow

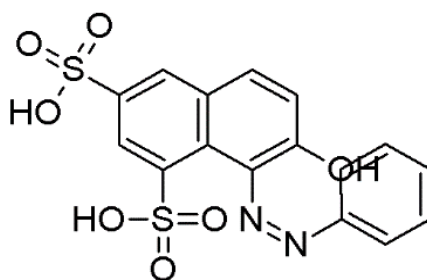


Figure A.12 Orange G

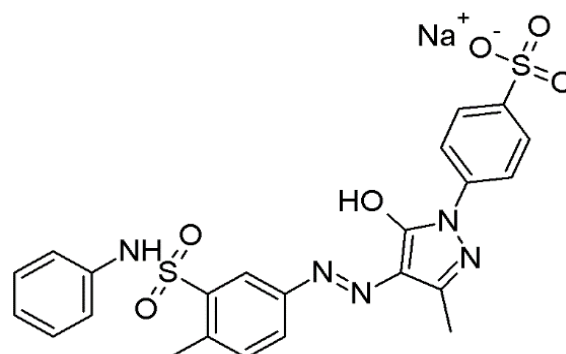


Figure A.13 Acid Yellow RN

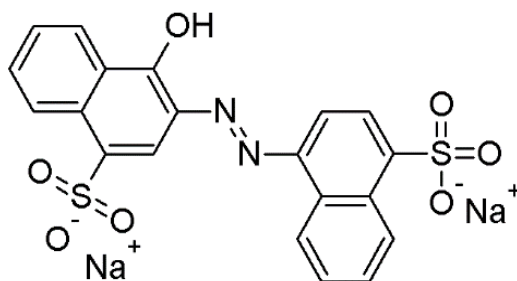


Figure A.14 Acid Brilliant Red B

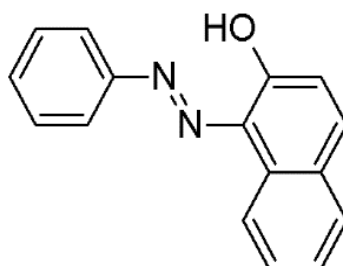


Figure A.15 1-(Phenylazo)-2-Naphthol

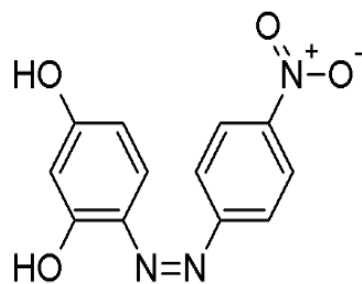


Figure A.16 4-(Nitrophenylazo) Resorcinol

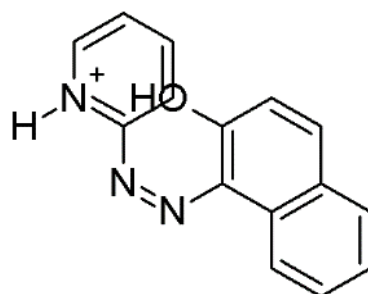


Figure A.17 1-(2-Pyridylazo)-2-Naphthol

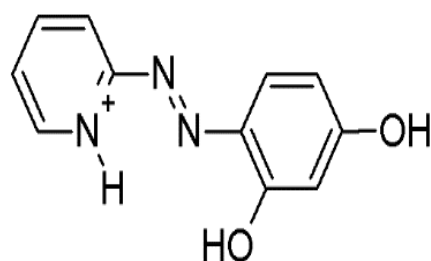


Figure A.18 4-(2-Pyridylazo) Resorcinol

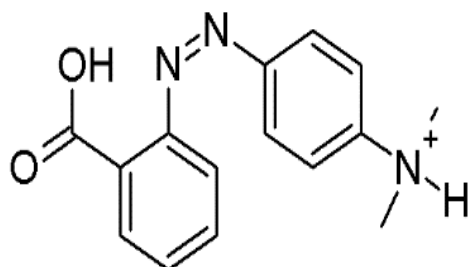


Figure A.19 Methyl Red

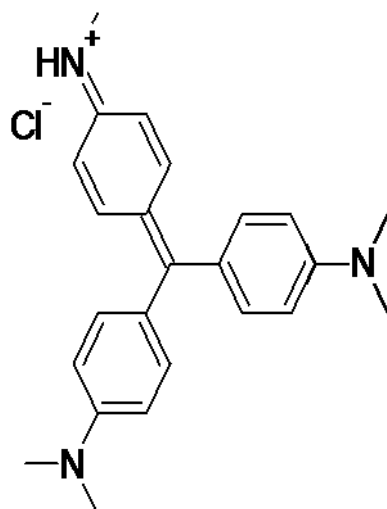
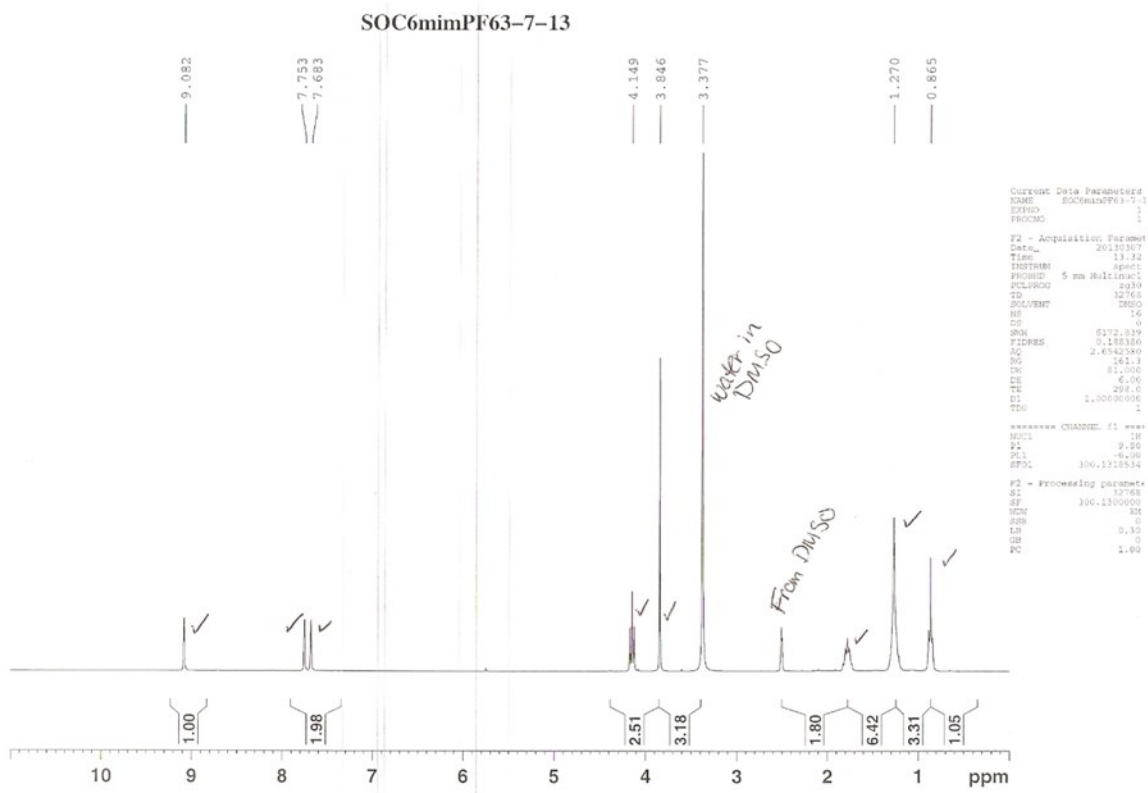


Figure A.20 Methyl Violet 2B

APPENDIX B

NMR Data

Figure B.1 NMR spectrum of C₆mimPF₆ in DMSO

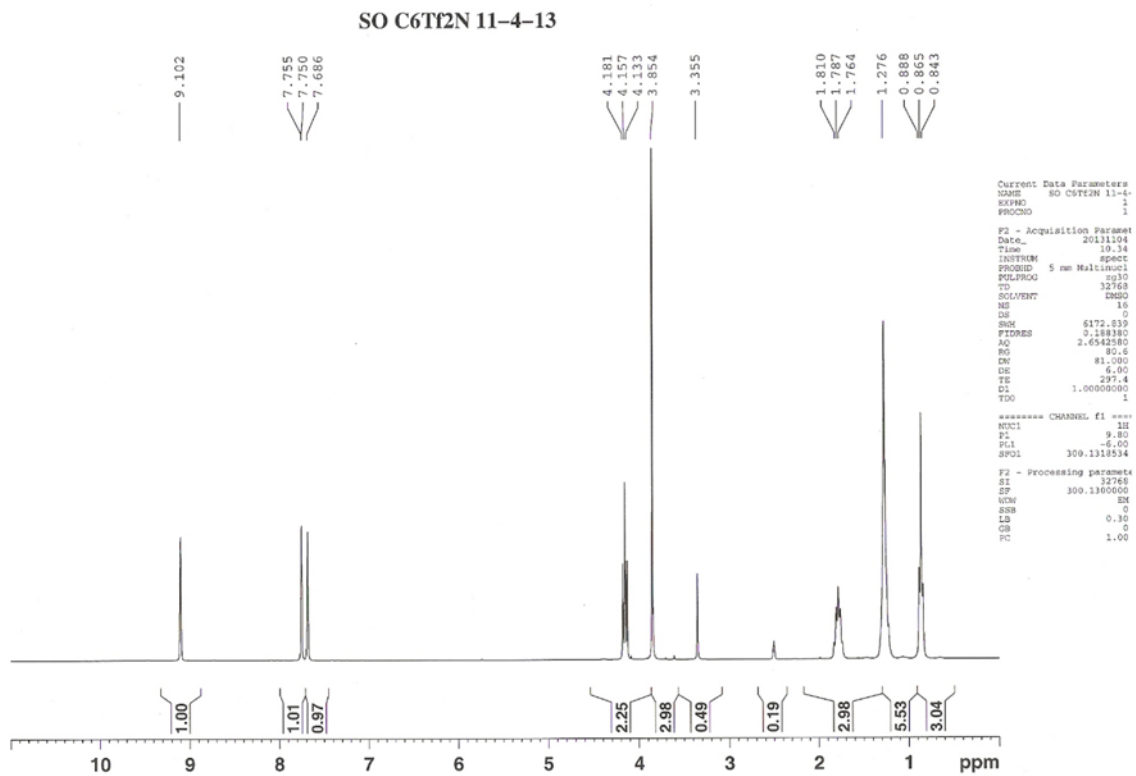


Figure B.2 NMR spectrum of C_6mimTf_2N in DMSO

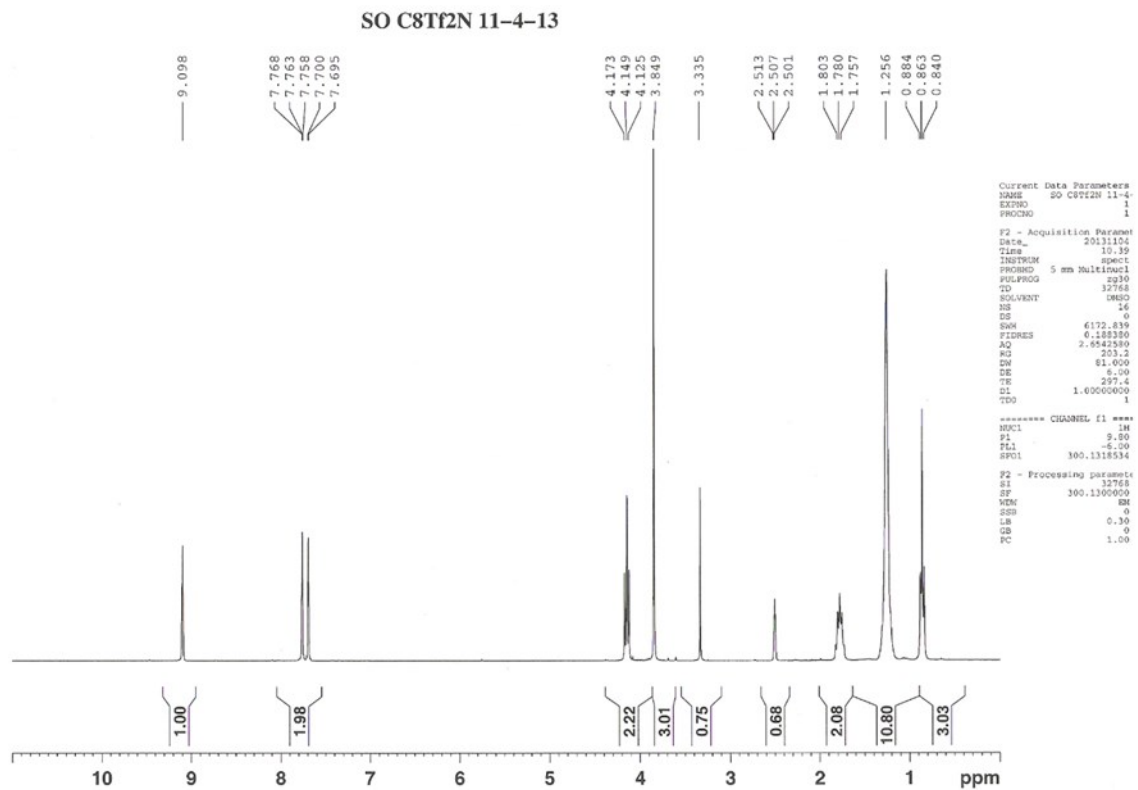


Figure B.3 NMR spectrum of C_8mimTf_2N in DMSO

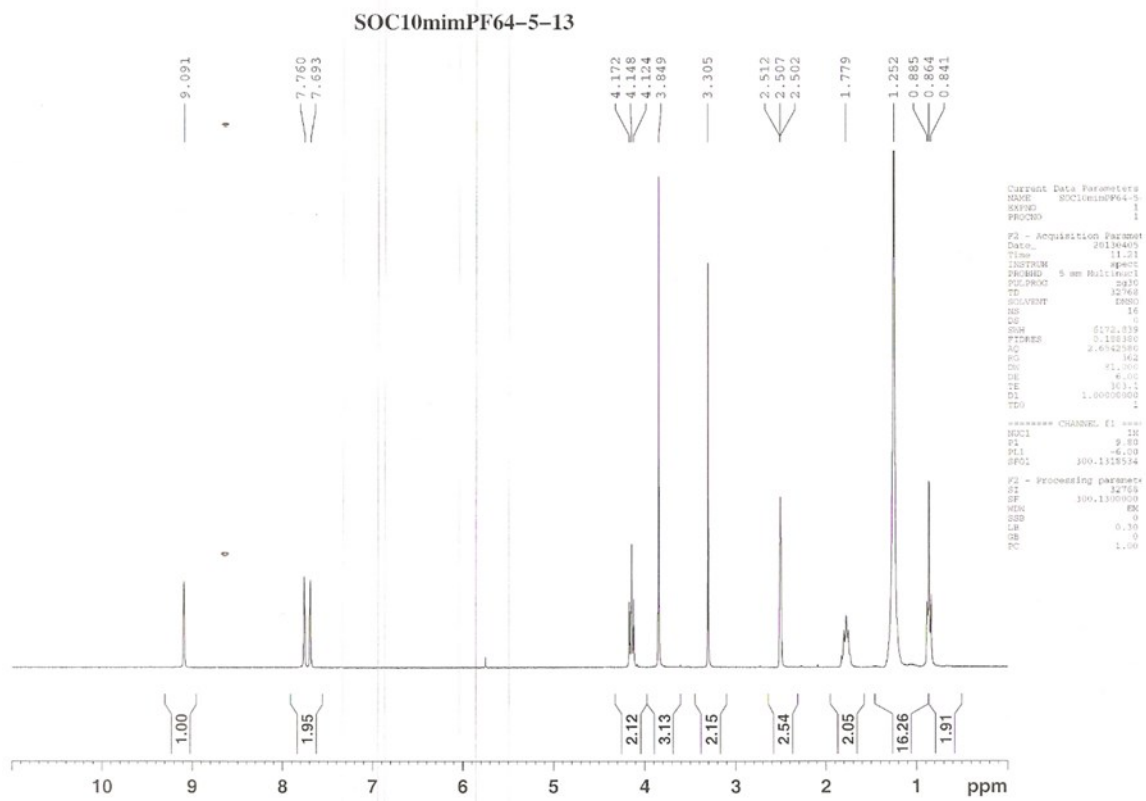


Figure B.4 NMR Spectrum of $C_{10}mimPF_6$ in DMSO

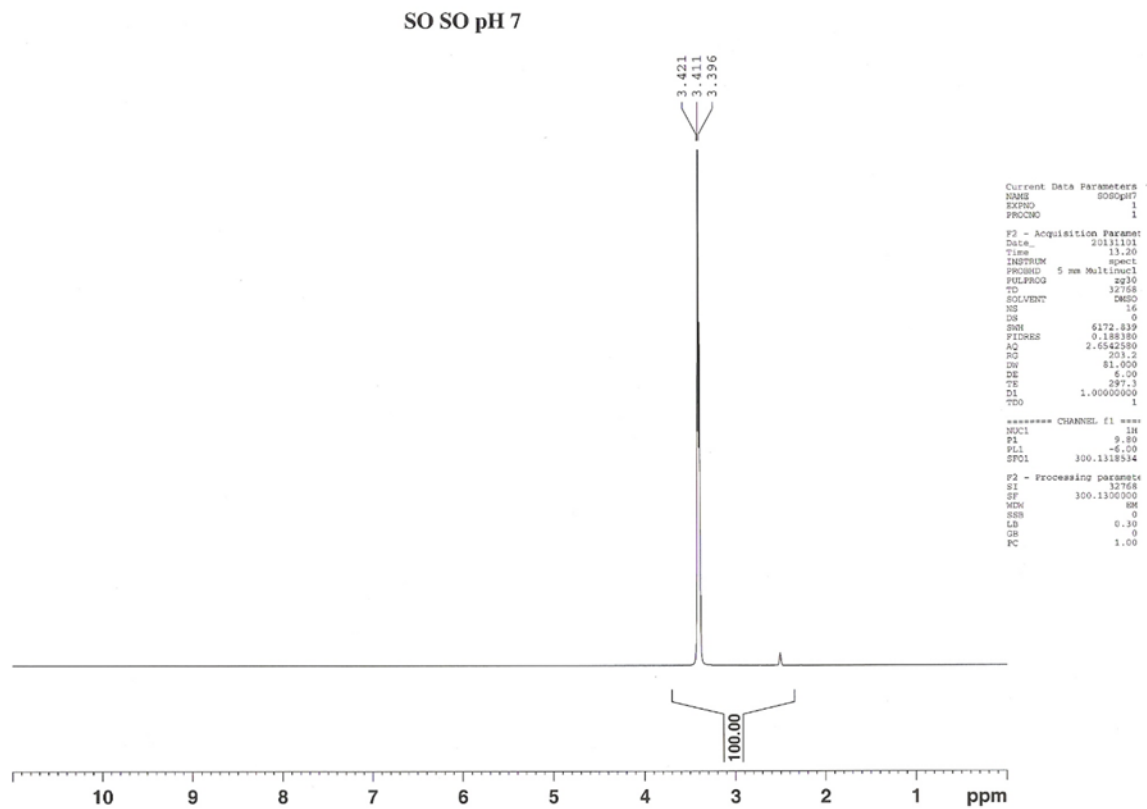


Figure B.5 NMR spectrum of Safranin O, pH 7, in DMSO

SO MV pH 7 11-2-13

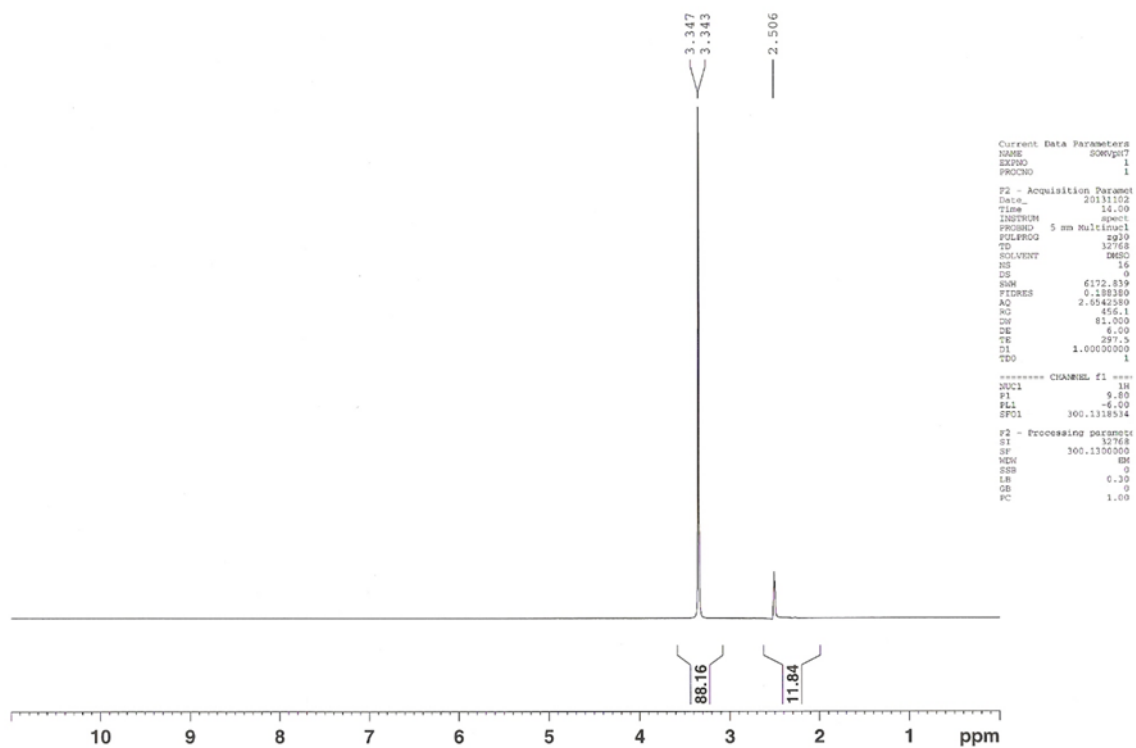


Figure B.6 NMR Spectrum of Methyl Violet, pH 7, in DMSO

SO SO 37 11-2-13

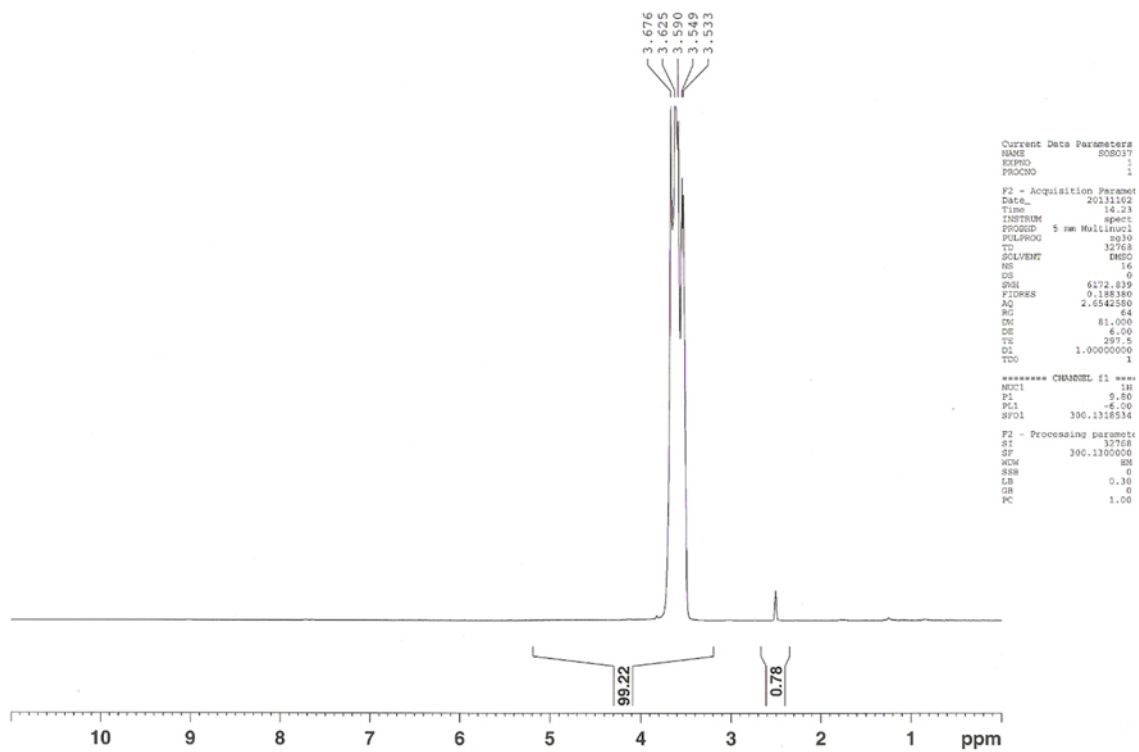


Figure B.7 NMR spectrum of aqueous phase of SO 37, pH 7, C₆mimPF₆

SO MV 43 11-2-13

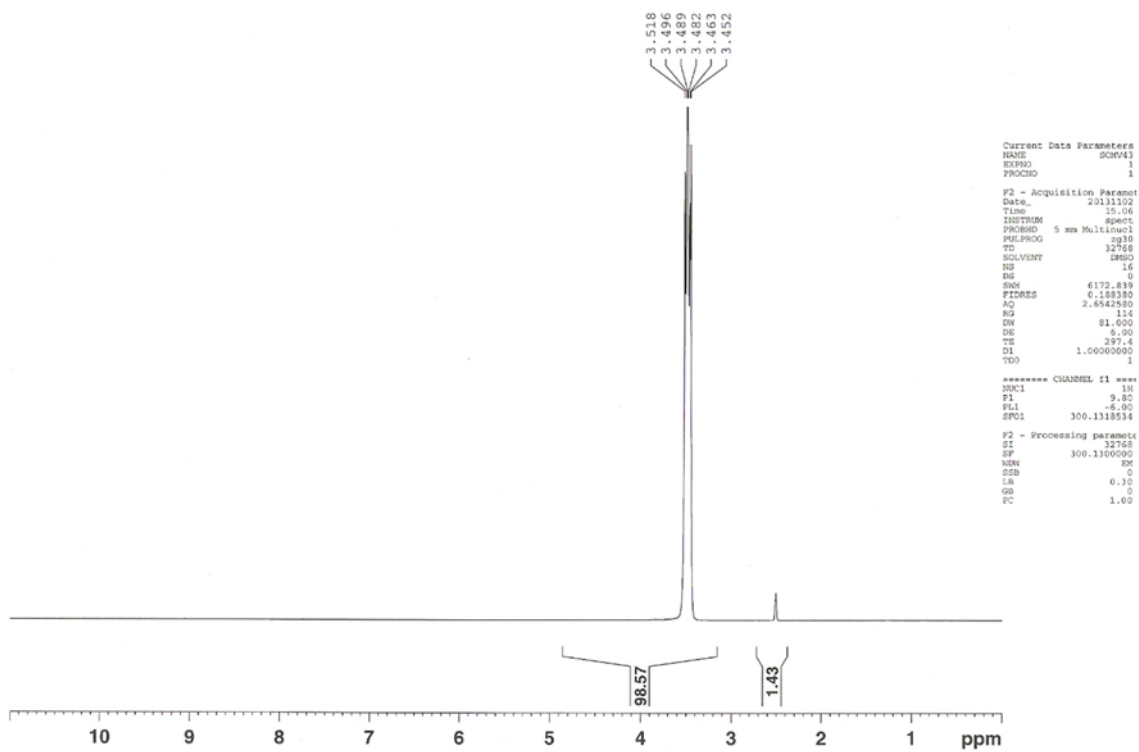


Figure B.8 NMR spectrum of aqueous phase of MV 43, pH 7, C₆mimTf₂N